Recognition of mixed-sequence dsDNA using LNA-modified toehold Invader probes

Shiva P. Adhikari, Philip Vukelich, Dale C. Guenther, Saswata Karmakar and Patrick J. Hrdlicka.

Department of Chemistry, University of Idaho, Moscow, ID-83844, USA

E-mail: hrdlicka@uidaho.edu

Electronic Supplementary Information

Definition of zipper nomenclature. The following nomenclature is used to describe the relative arrangement between two monomers on opposing strands in a duplex. The number *n* describes the distance measured in number of base pairs and has a positive value if a monomer is shifted toward the 5′-side of its strand relative to a second reference monomer on the other strand. Conversely, *n* has a negative value if a monomer is shifted toward the 3′-side of its strand relative to a second reference monomer on the other strand.

Table S1. MS data of ONs used in this study.[a]

ON	Sequence	Calculated *m/z* $(M+H)^+$	Observed *m/z* $(M+H)^+$
1[b]	5'-GGTA**U**A**U**ATAGGC	4446.0	4447.5
2[b]	3'-CCATA**U**A**U**ATCCG	4326.0	4327.0
3	5'-ACA-GGTA**U**A**U**ATAGGC	5362.0	5362.0
4	3'-CCATA**U**A**U**ATCCG-GCG	5274.0	5274.0
5	5'-A**C**A-GGTA**U**A**U**ATA-GGC	5592.0	5591.0
6	3'-CCATA**U**A**U**ATCCG-G**C**G	5504.0	5505.5
7	5'-TGCACA-GGTA**U**A**U**ATAGGC	6284.5	6284.0
8	3'-CCATA**U**A**U**ATCCGGCG-TAT	6195.0	6195.0
9	5'-**U**GCA**C**A-GGTA**U**A**U**ATAGGC	6731.0	6731.5
10	3'-CCATA**U**A**U**ATCCG-G**C**GTA**U**	6642.0	6642.5
11	5'-**U**GCACA-GGTATATATAGGC	6298.5	6300.0
12	3'-CCATATATATCCG-G**C**GTA**U**	6209.5	6210.0
15	5'-GGTA**U**A**U**ATAGGC-**C**GCA**U**A	6731.0	6732.0
16	3'-A**C**GTG**U**-CCATA**U**A**U**ATCCG	6642.0	6642.5
17	5'-**t**GCA**c**A-GGTA**U**A**U**ATAGGC	6354.0	6354.0
18	3'-CCATA**U**A**U**ATCCG-G**c**GTA**t**	6265.5	6266.0
19	5'-**t**G**c**AC**a-**GG**U**A**U**ATA**U**AGGC	6598.5	6599.5
20	3'-CCA**U**A**U**ATA**U**CCG-**g**CG**t**A**t**	6495.5	6497.0
DYZ-OPTu	5'-Cy3-T**g**T**g**TGT**U**A**U**ATGCTG**U**TCTC'	7636.0	7637.0
DYZ-OPTd	3'- AA**U**A**U**ACGACA**A**GAGTC**g**G**g**A-Cy3	7738.0	7737.5

[a] All reported data are determined from MALDI-MS except for **DYZ-OPTu** and **DYZ-OPTd** (LC-ESI-MS).

[b] Data previously reported in reference S1.

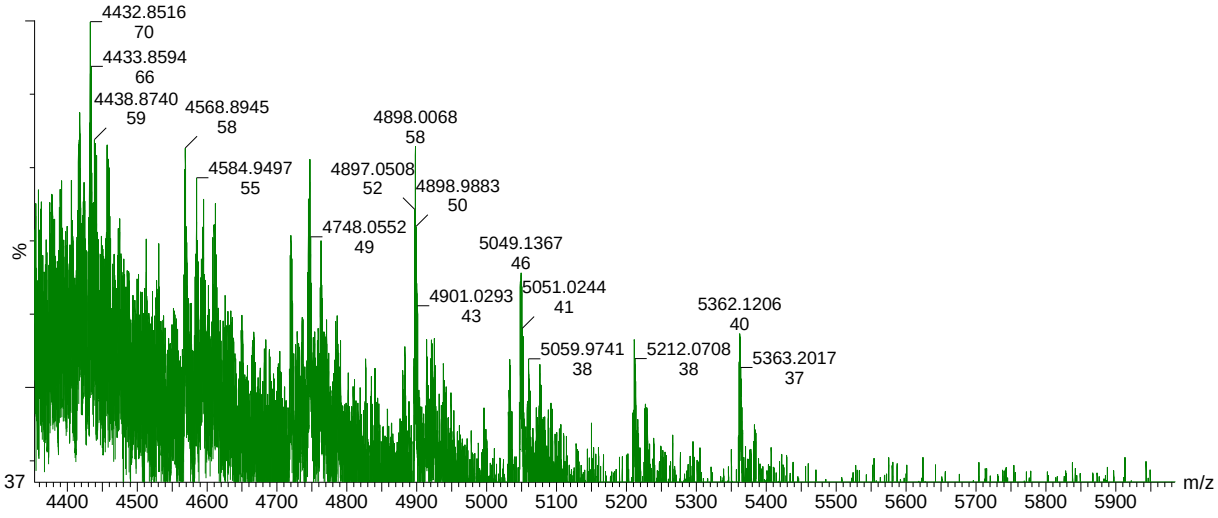

Figure S1. MALDI-MS spectrum of **ON3**.

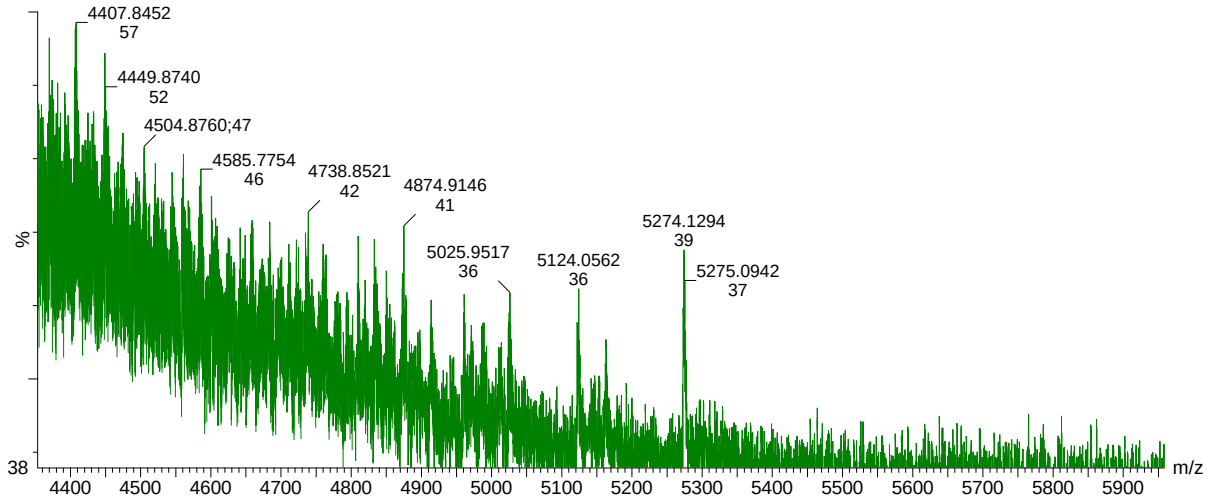

Figure S2. MALDI-MS spectrum of **ON4**.

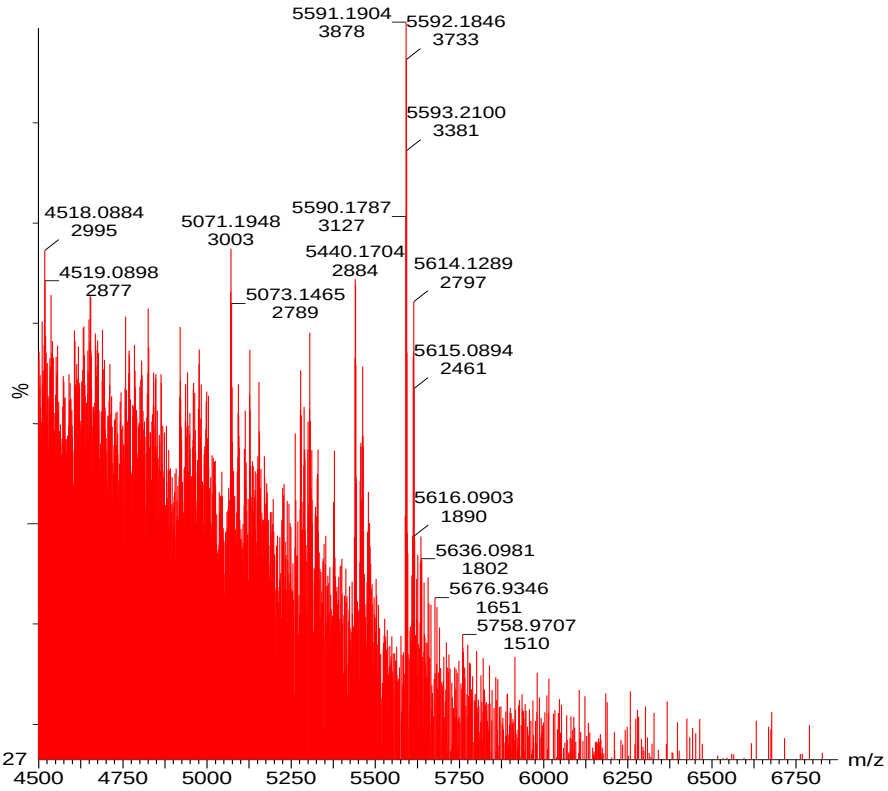

Figure S3. MALDI-MS spectrum of **ON5**.

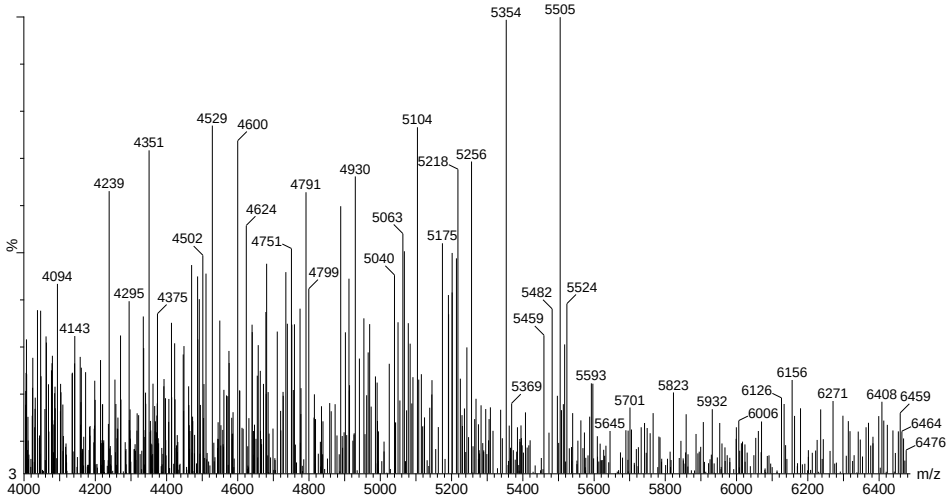

Figure S4. MALDI-MS spectrum of **ON6**.

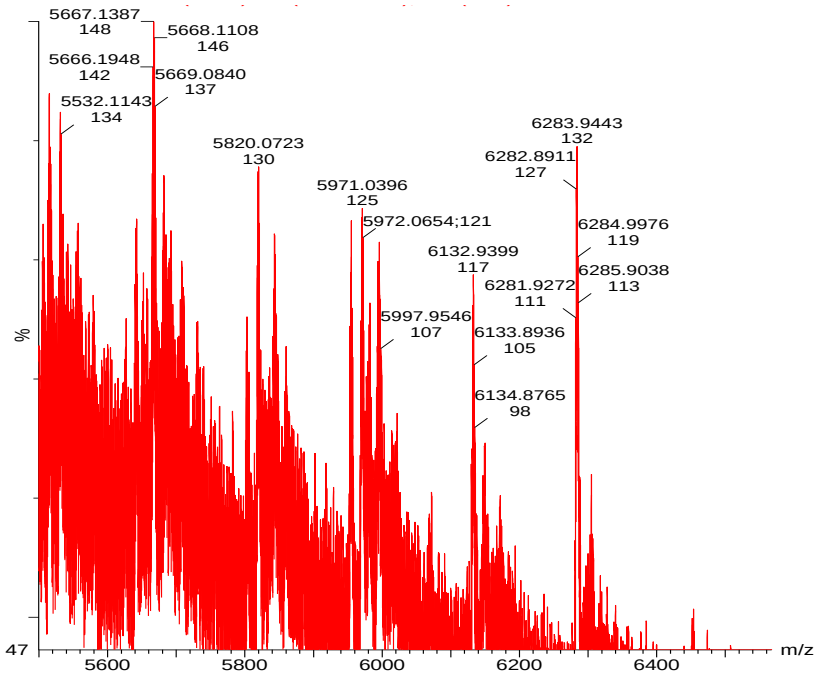

Figure S5. MALDI-MS spectrum of **ON7**.

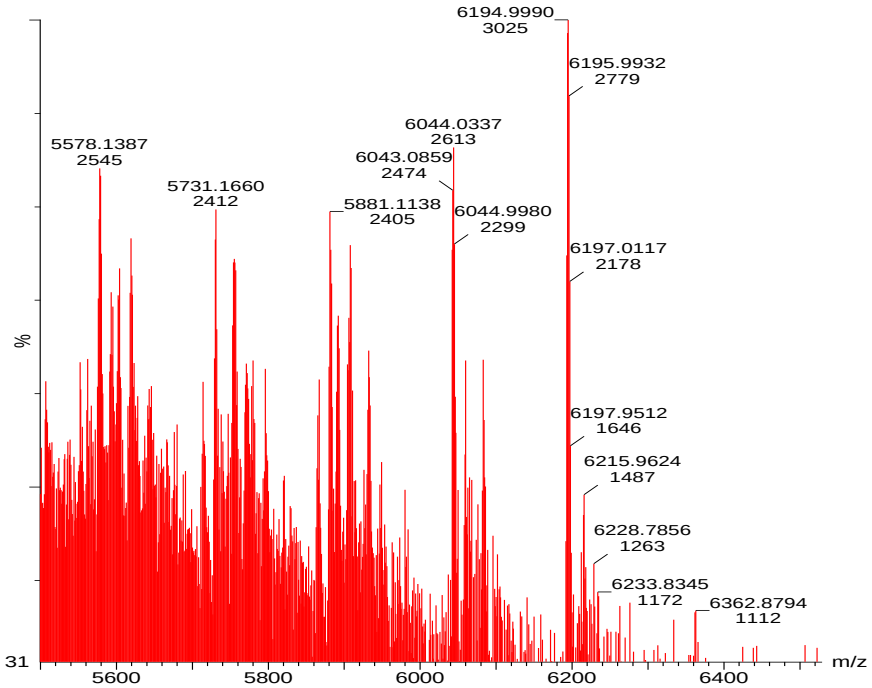

Figure S6. MALDI-MS spectrum of **ON8**.

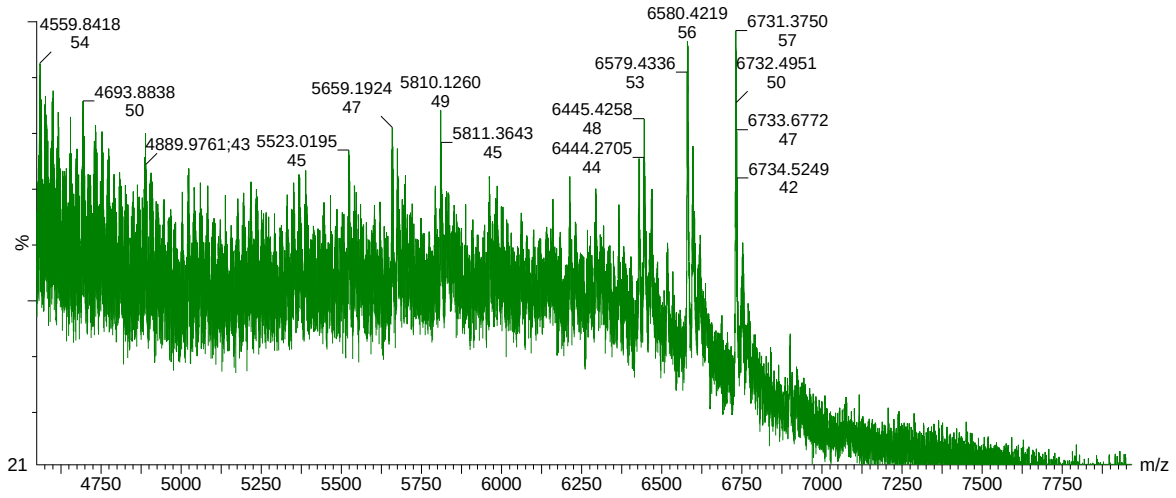

Figure S7. MALDI-MS spectrum of **ON9**.

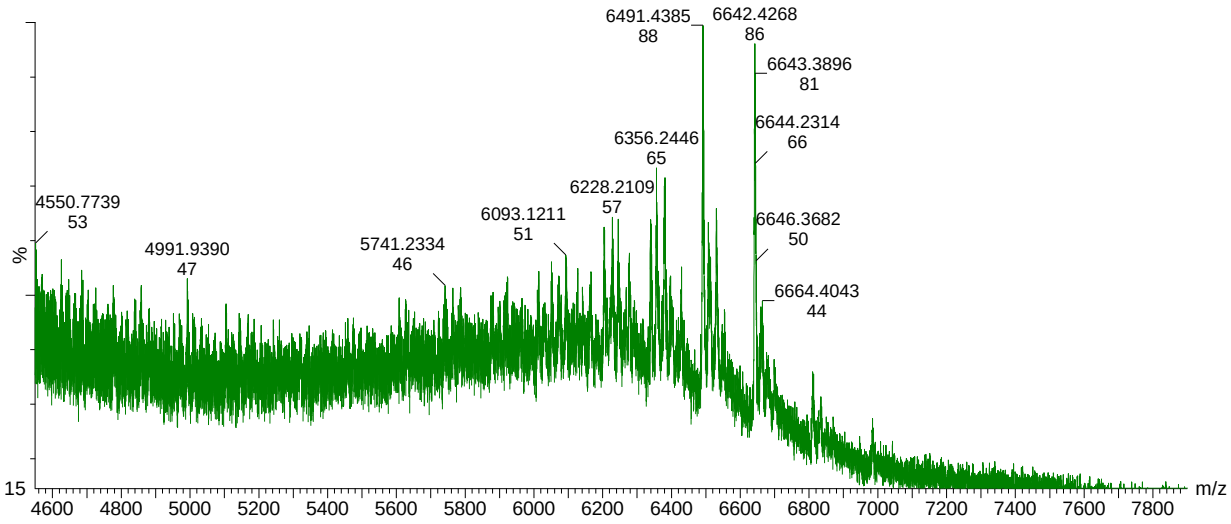

Figure S8. MALDI-MS spectrum of **ON10**.

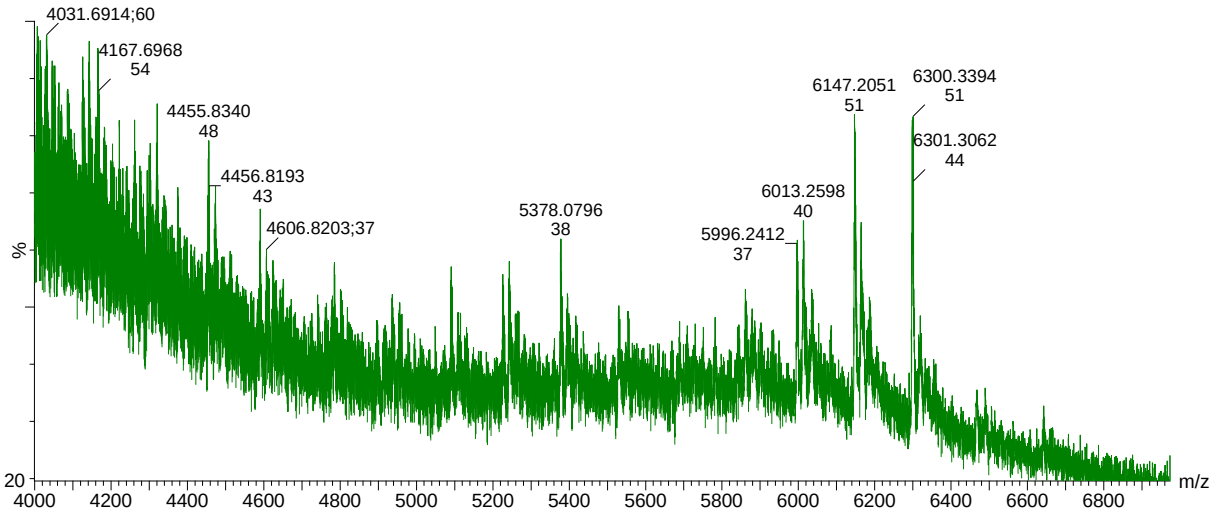

Figure S9. MALDI-MS spectrum of **ON11**.

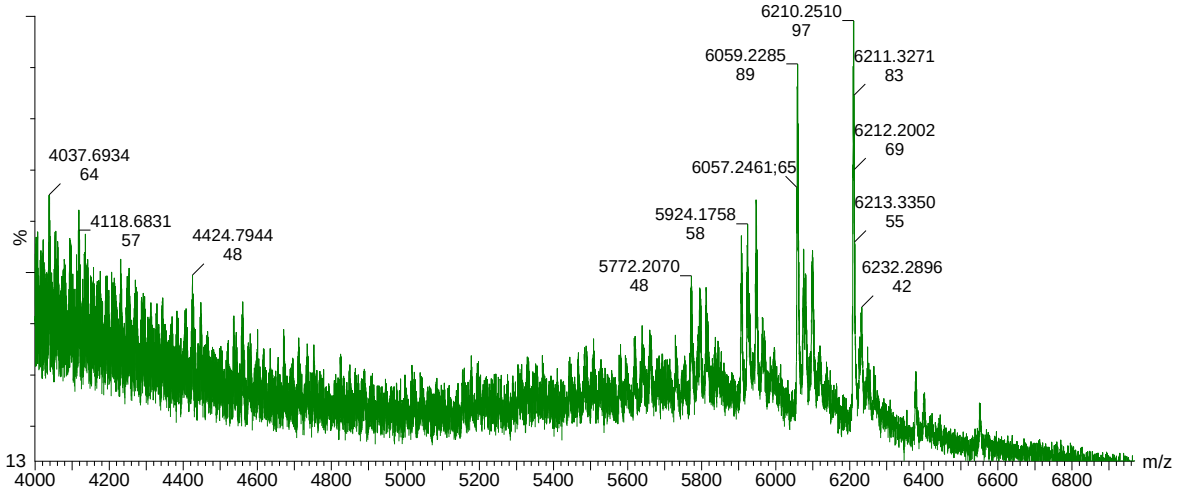

Figure S10. MALDI-MS spectrum of **ON12**.

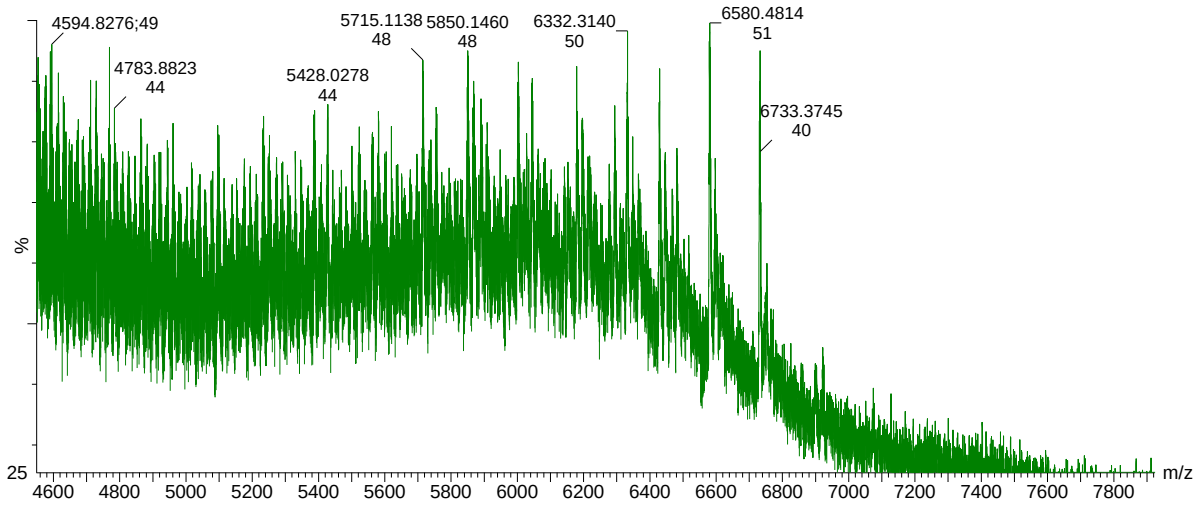

Figure S11. MALDI-MS spectrum of **ON15**.

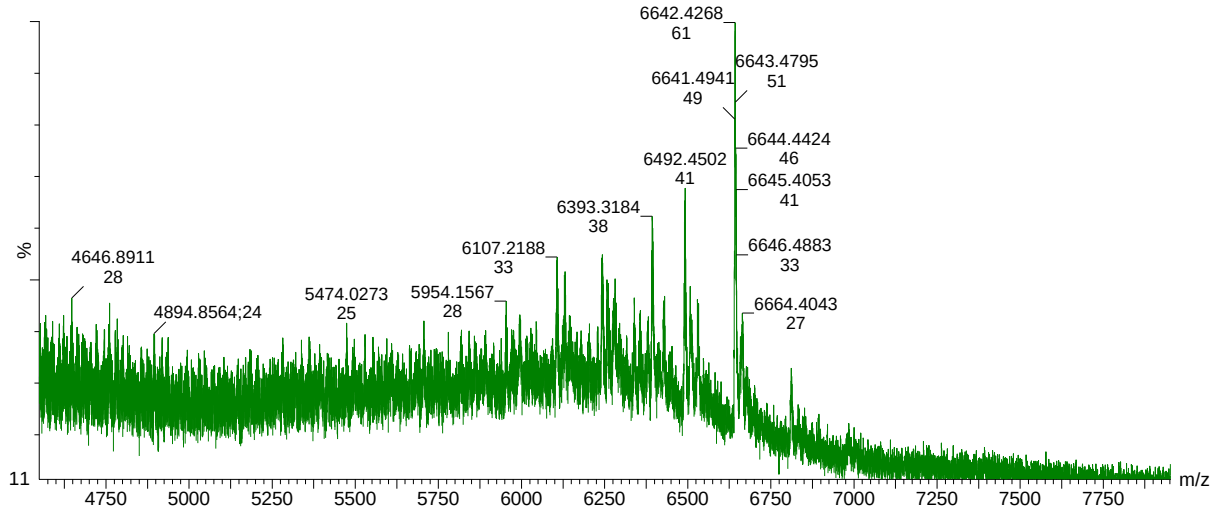

Figure S12. MALDI-MS spectrum of **ON16**.

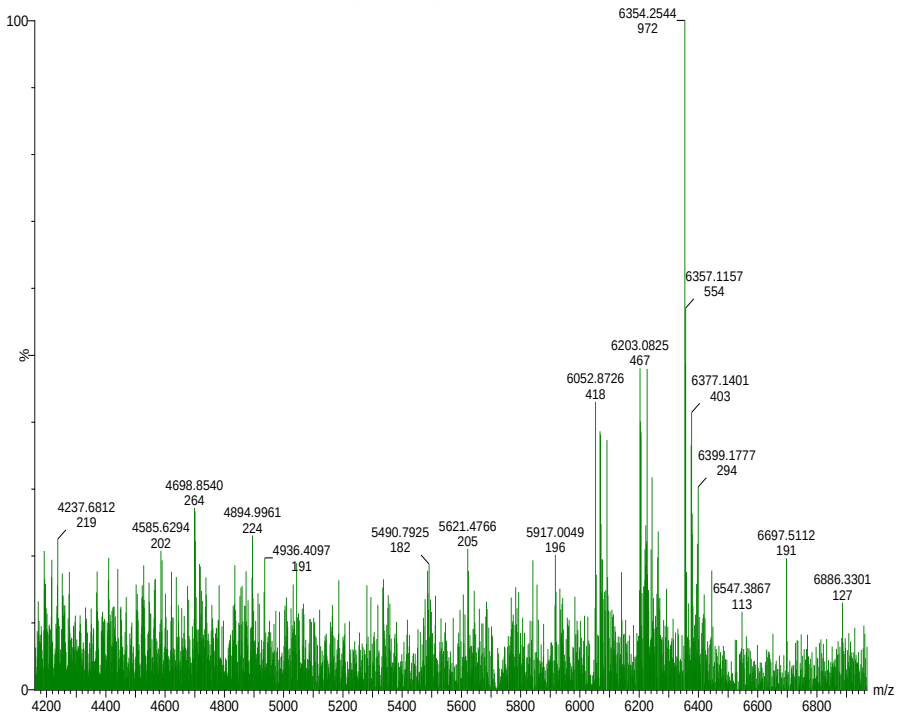

Figure S13. MALDI-MS spectrum of **ON17**.

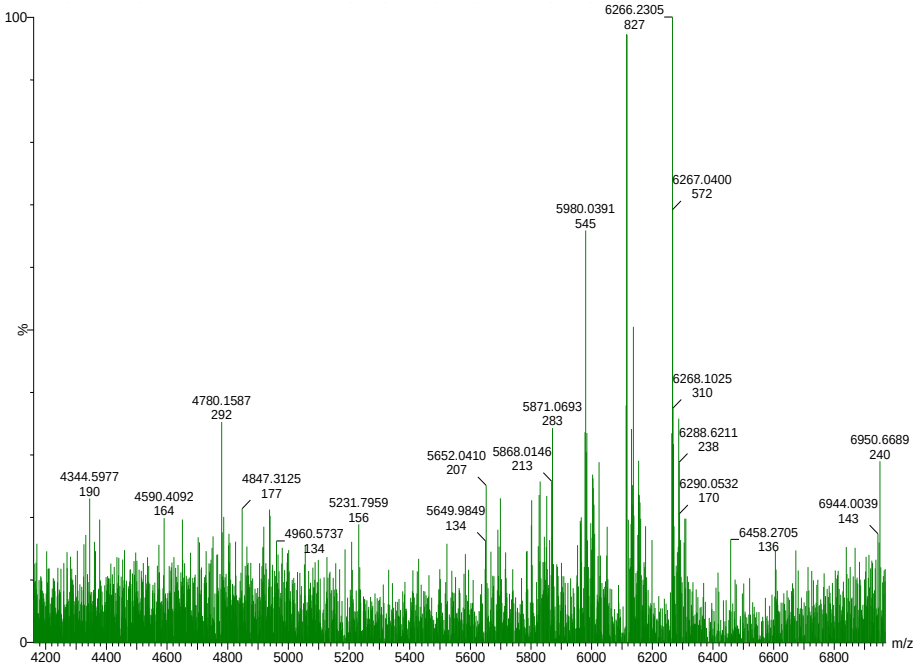

Figure S14. MALDI-MS spectrum of **ON18**.

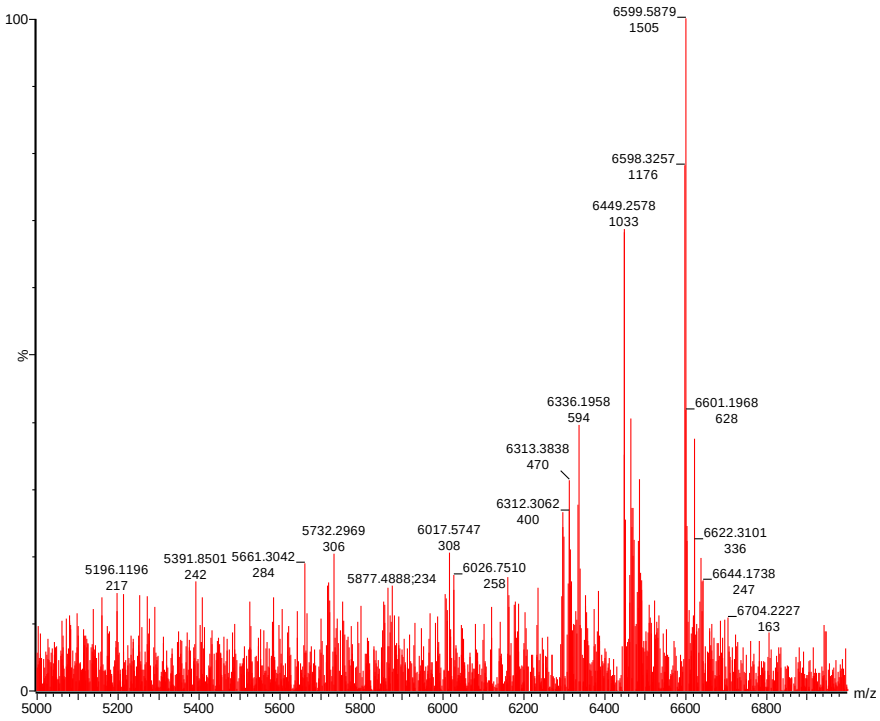

Figure S15. MALDI-MS spectrum of **ON19**.

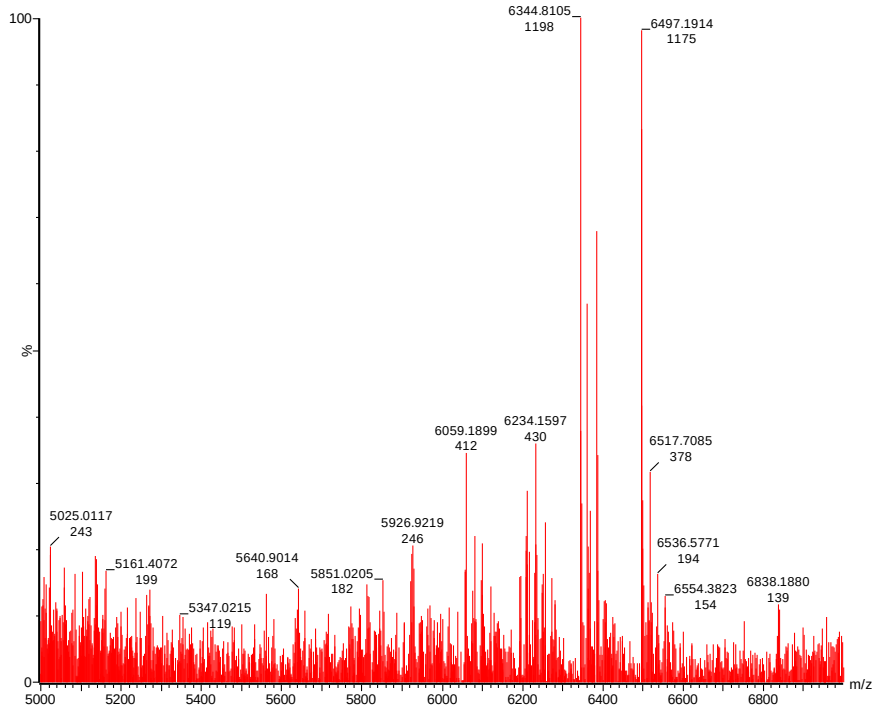

Figure S16. MALDI-MS spectrum of **ON20**.

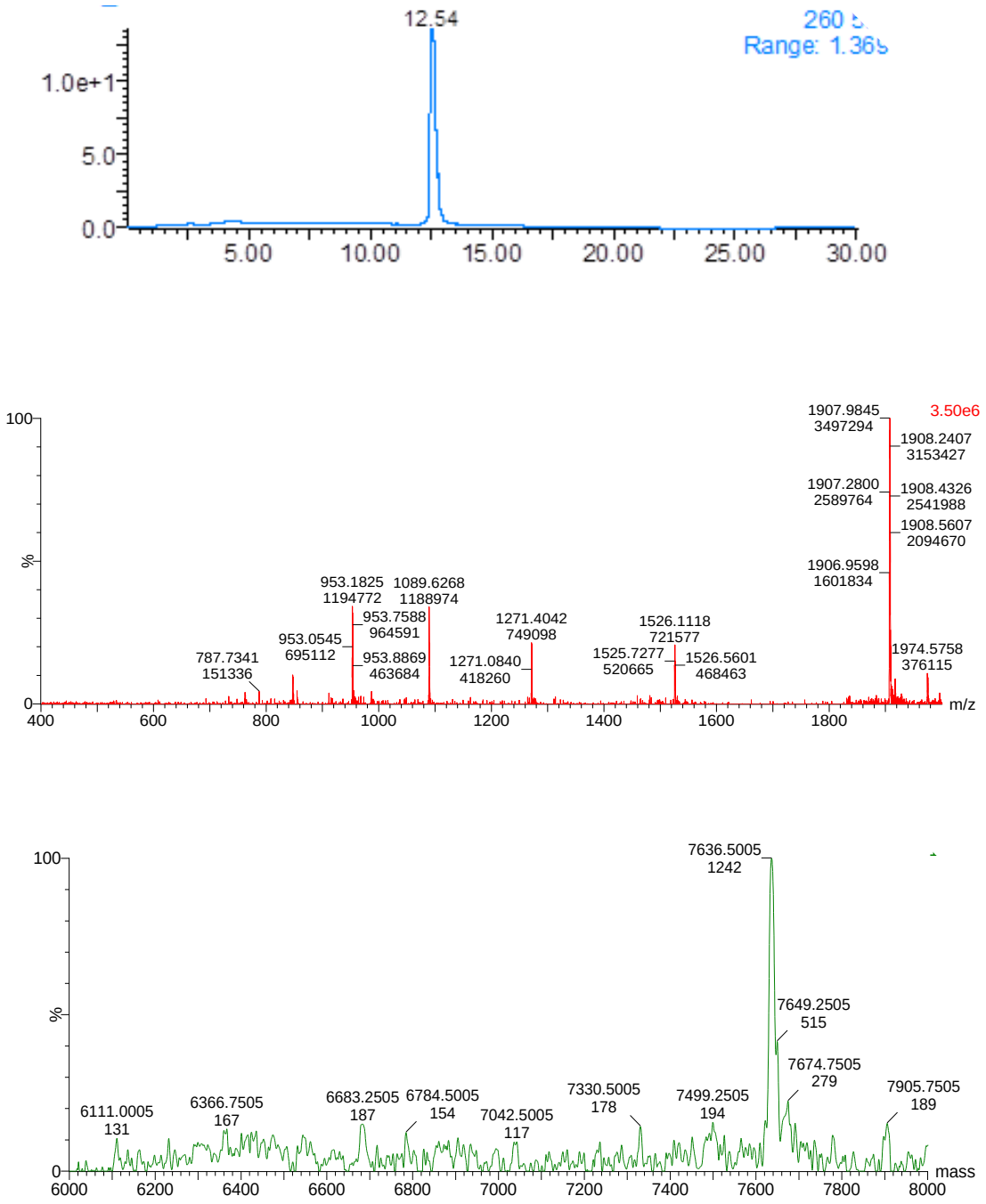

Figure S17. LC-ESI-MS analysis of **DYZ-OPTu**. LC-trace (upper panel), unprocessed (middle panel) and deconvoluted (lower panel) MS spectrum.

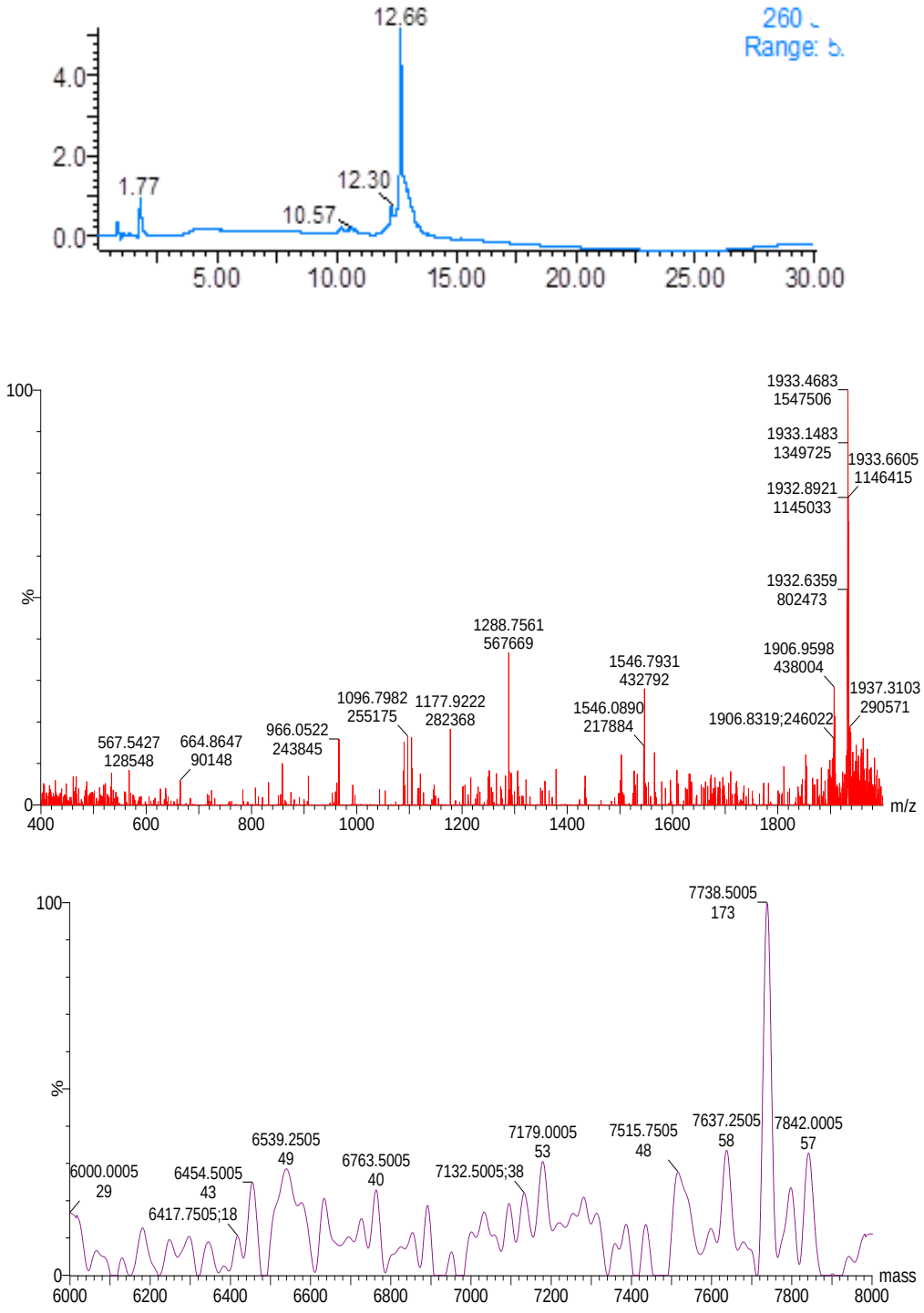

Figure S18. LC-ESI-MS analysis of **DYZ-OPTd**. LC trace (upper panel), unprocessed (middle panel) and deconvoluted (lower panel) MS spectrum.

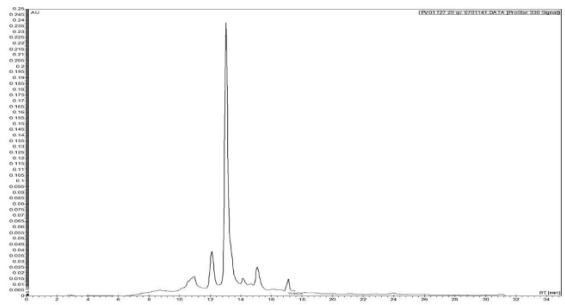

ON3

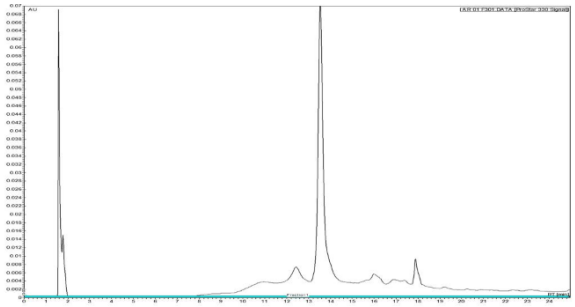

ON7

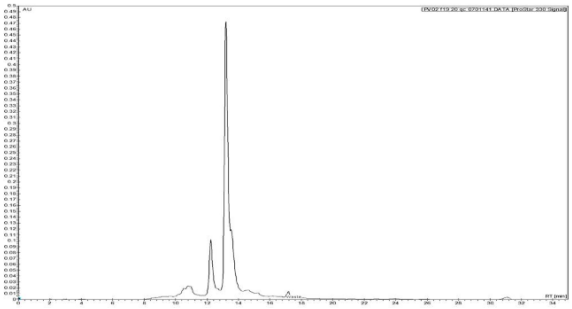

ON4

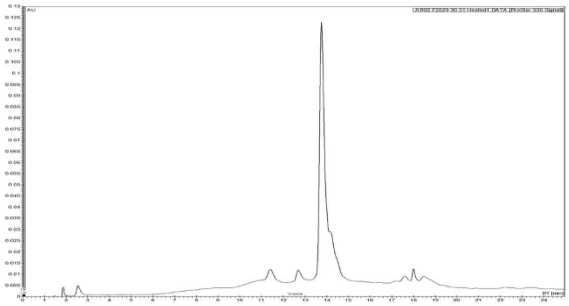

ON8

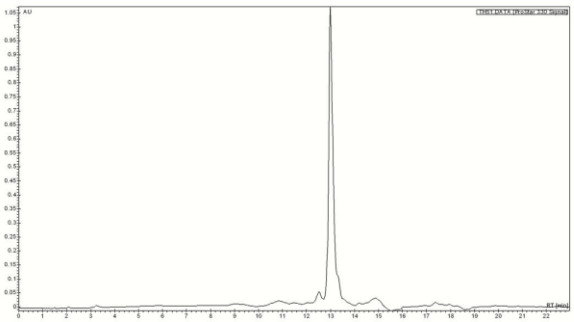

ON5

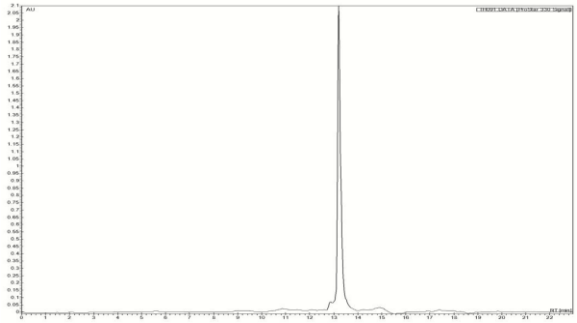

ON9

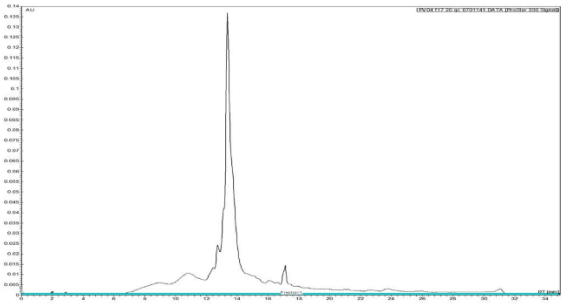

ON6

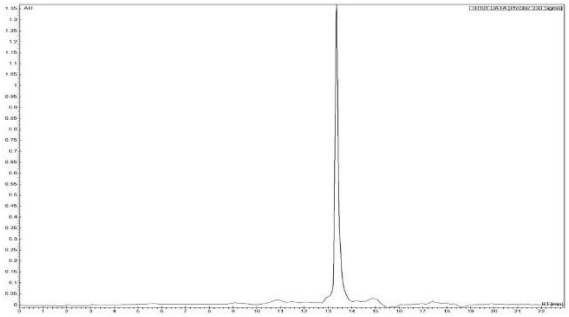

ON10

Figure S19. HPLC traces of **ON3**-**ON10**.

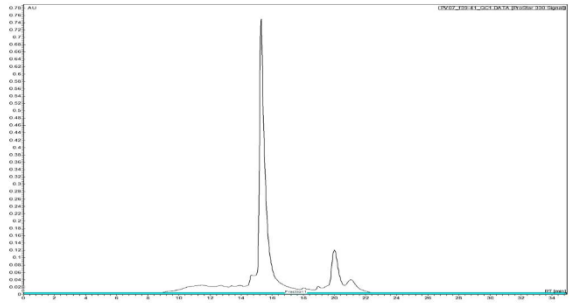

ON11

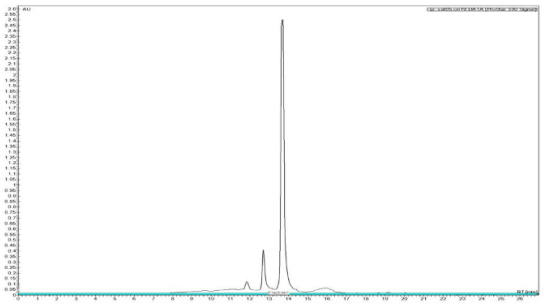

ON17

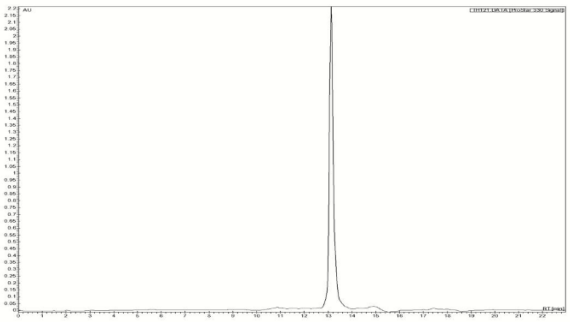

ON12

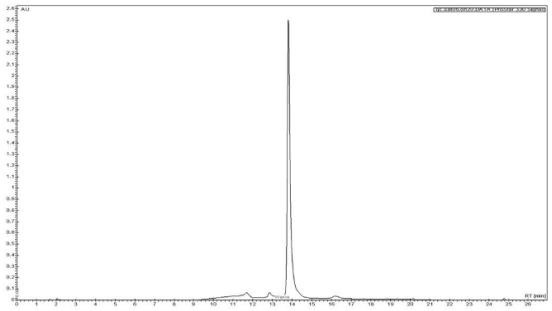

ON18

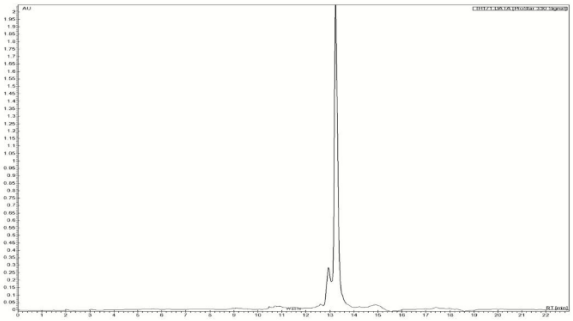

ON15

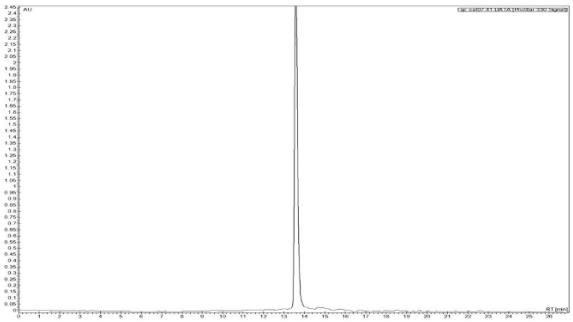

ON19

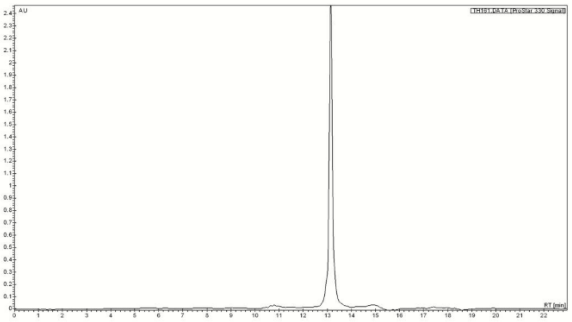

ON16

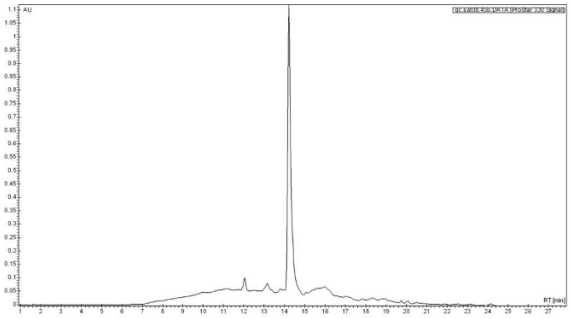

ON20

Figure S20. HPLC traces of **ON11**, **ON12**, **ON15**, **ON16**, and **ON17-ON20**.

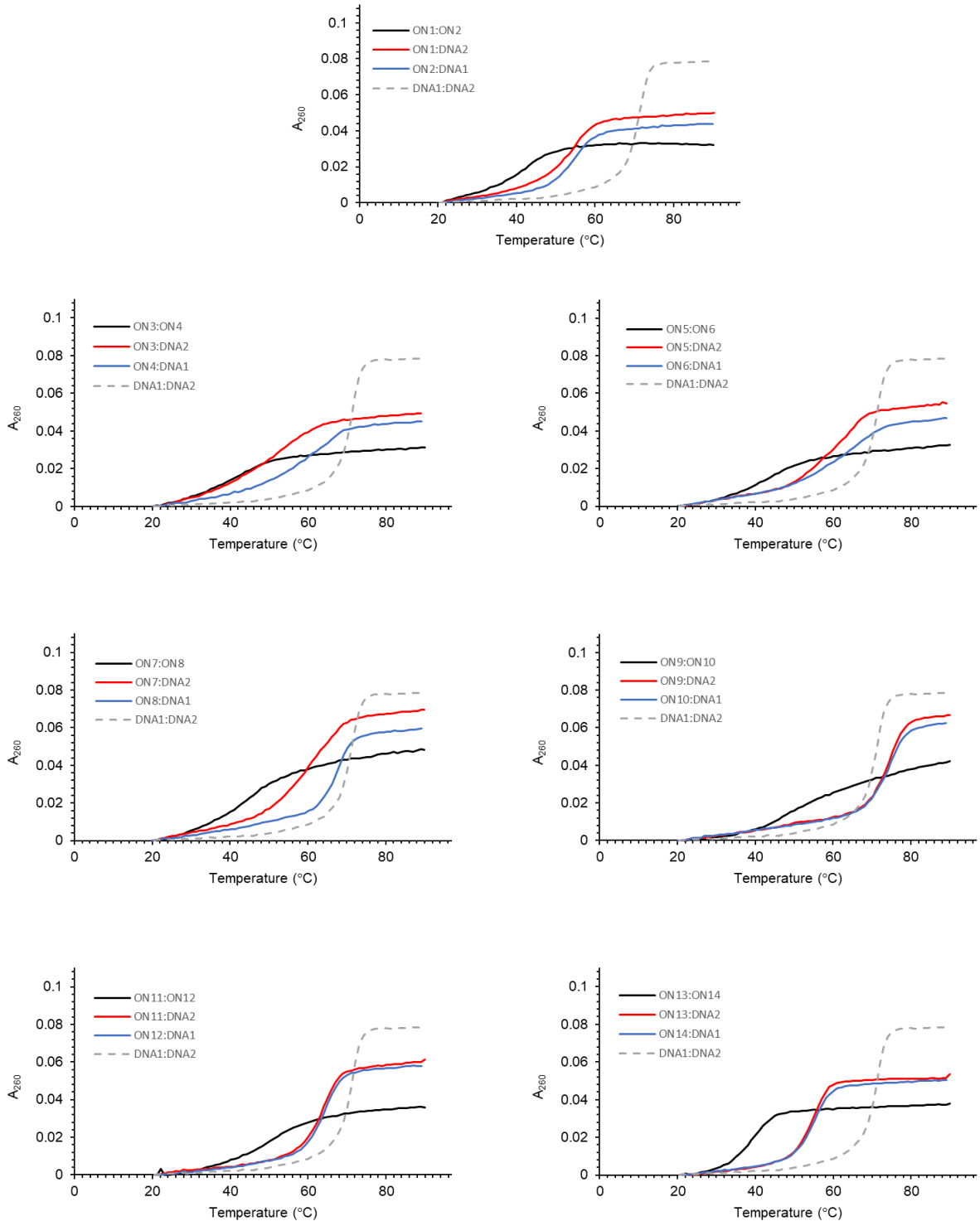

Figure S21. Representative thermal denaturation curves of double-stranded probes (**ON1**:**ON2**-**ON13**:**ON14**), duplexes between individual probe strands and single-stranded 33-mer DNA strands **DNA1** or **DNA2**, and model dsDNA target **DNA1**:**DNA2**. For experimental conditions, see Table 1.

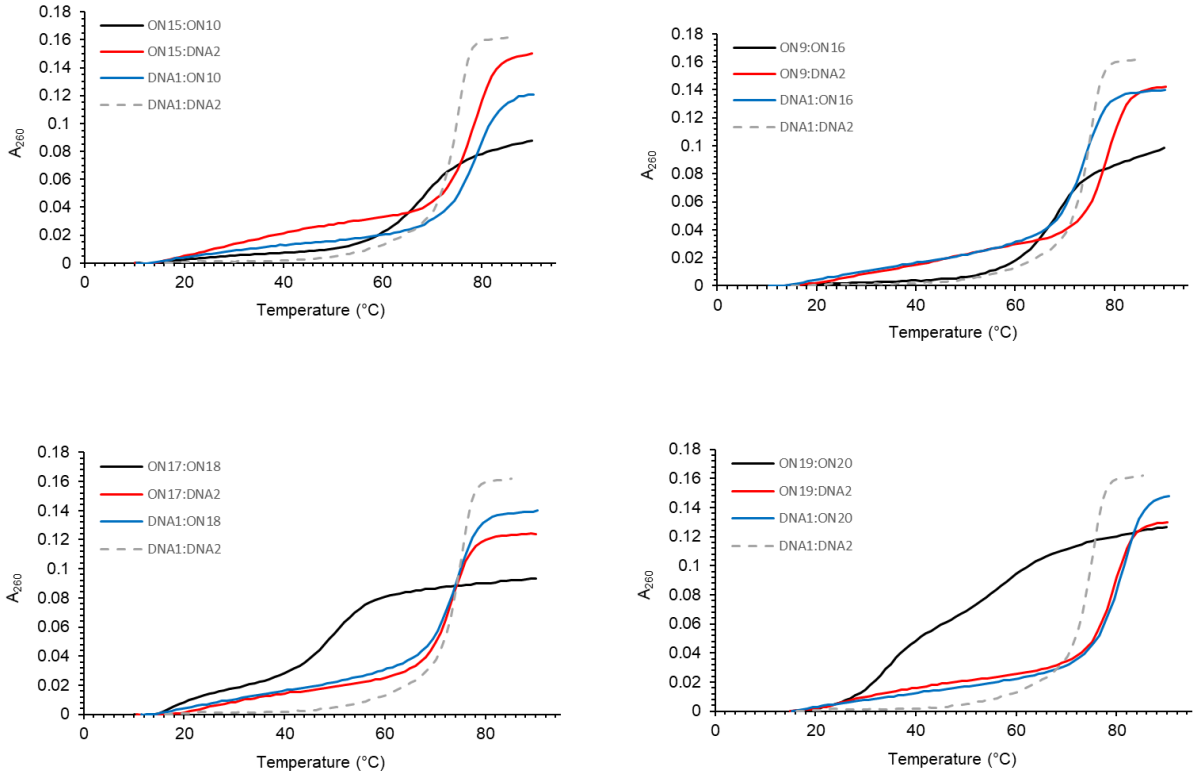

Figure S22. Representative thermal denaturation curves of Invader probes (**ON15**:**ON10**, **ON9**:**ON16**, **ON17**:**ON18**, and **ON19**:**ON20**), duplexes between individual probe strands and single-stranded 33-mer DNA strands **DNA1** or **DNA2**, and model dsDNA target **DNA1**:**DNA2** in medium salt buffer. For experimental conditions, see Table 1.

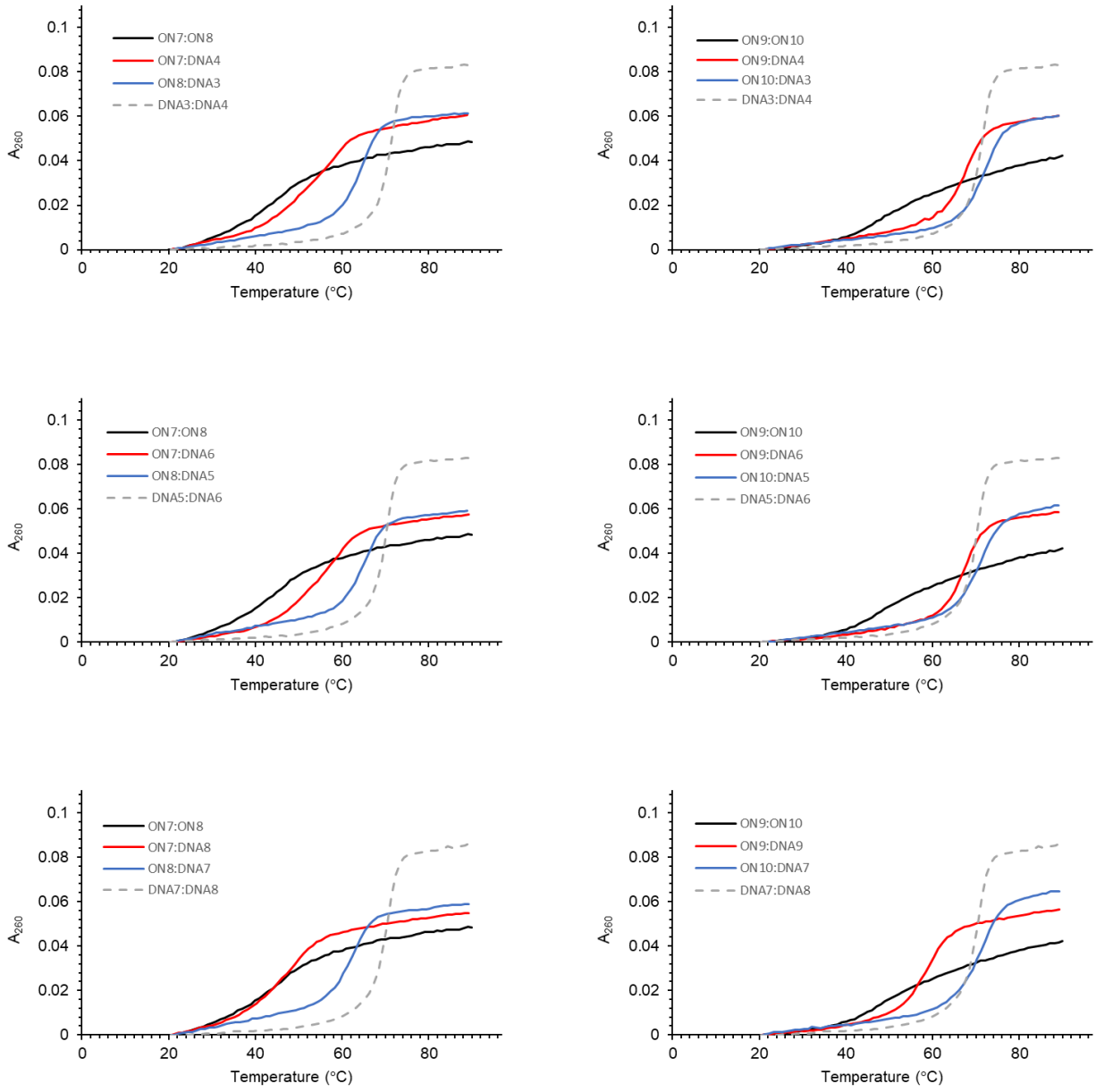

Figure S23. Representative thermal denaturation curves for Invader probes **ON7**:**ON8** and **ON9**:**ON10**, mismatched duplexes between individual probe strands and single-stranded non-target DNA strands, and **DNA3**:**DNA4**, **DNA5**:**DNA6** and **DNA7**:**DNA8**, which differ in sequence at one, two and three positions respectively, relative to **DNA1**:**DNA2** (for sequences of the mismatched dsDNA and tabulated data, see Tables S6 and S7). For experimental conditions, see Table 1.

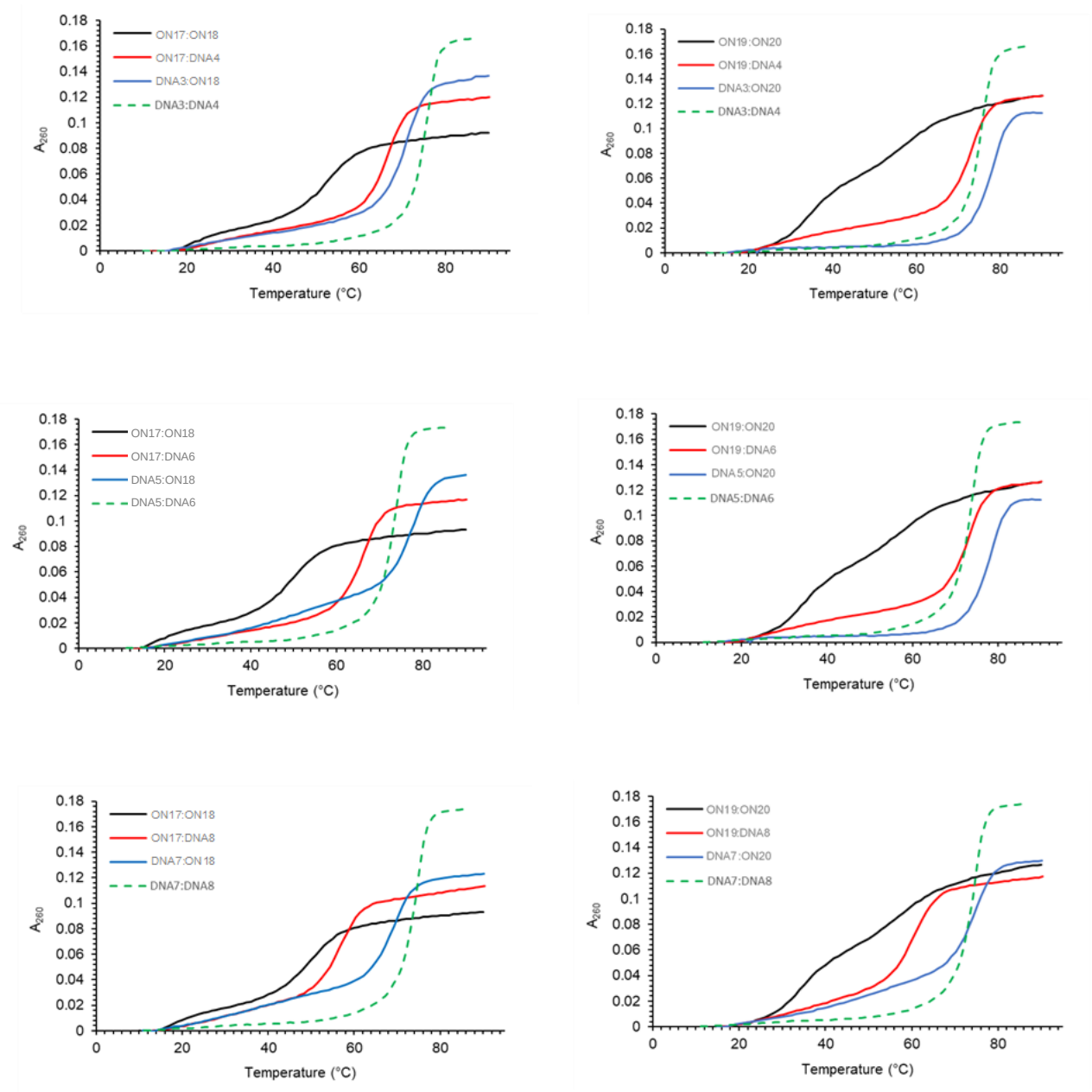

Figure S24. Representative thermal denaturation curves for Invader probes **ON17**:**ON18** and **ON19**:**ON20**, mismatched duplexes between individual probe strands and single-stranded non-targeted DNA strands, and **DNA3**:**DNA4**, **DNA5**:**DNA6** and **DNA7**:**DNA8**, which differ in sequence at one, two and three positions respectively, relative to **DNA1**:**DNA2** (for sequences of the mismatched dsDNA and tabulated data, see Tables S10 & S11). For experimental conditions, see Table 1.

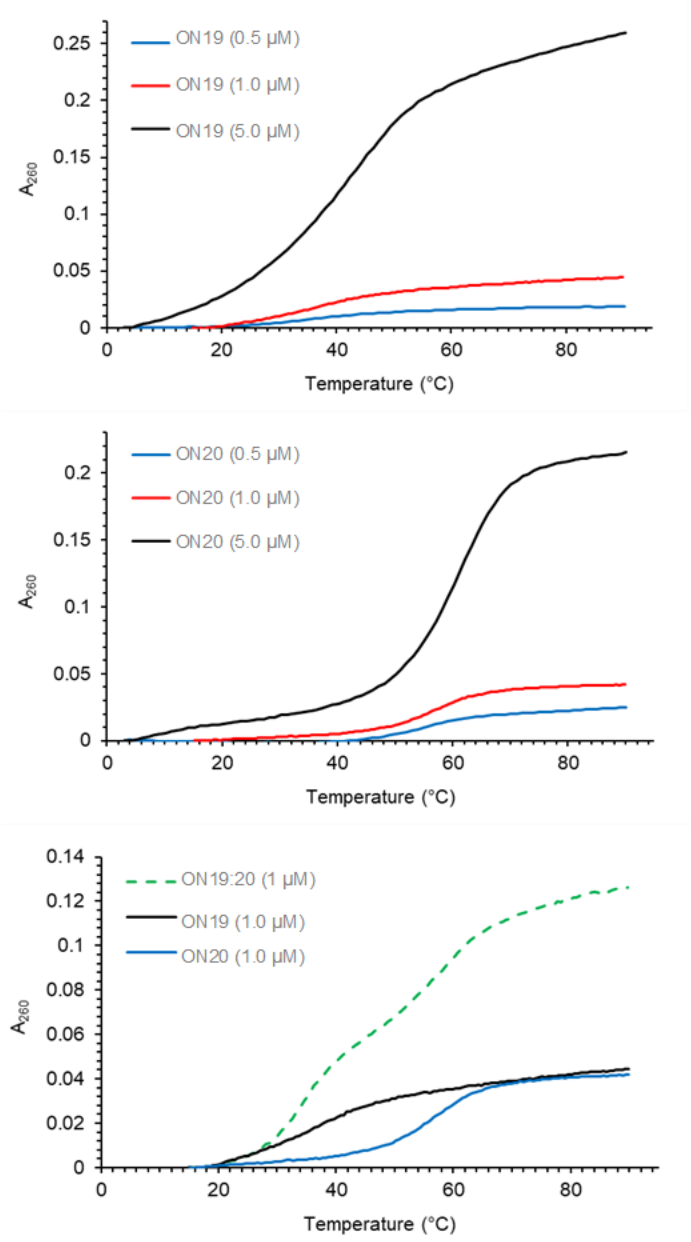

Figure S25. Representative thermal denaturation curves of individual Invader probe strands **ON19** and **ON20** at different concentrations in medium salt buffer (upper and middle panels) and of probe strands **ON19** and **ON20** as compared to **ON19**:**ON20** at 1 μM concentration (lower panel). For experimental conditions, see Table 1.

TA-based discussion of dsDNA-recognition potential of probes. The driving force for recognition of the 33-mer model dsDNA target **DNA1**:**DNA2** by double-stranded probes can be estimated by the term *thermal advantage*, defined as *TA* = T_m (5'-probe vs **DNA2**) + T_m (3'-probe strand vs **DNA1**) - T_m (probe duplex) - T_m (**DNA1**:**DNA2**), with large positive values indicative of a probe that is strongly activated for dsDNA-recognition (Table 1).[S2] The *TA*-based conclusions presented in the following generally align with the ΔG^{310}_{rec}-based conclusions discussed in the main manuscript (Table 2). Thus, the 13-mer conventional Invader probe **ON1**:**ON2** is not sufficiently activated to facilitate recognition of the 33-mer model dsDNA target (*TA* = -6 °C, Table 1). Invader probe **ON3**:**ON4**, which features unmodified 3-mer overhangs, is minimally activated for DNA recognition (*TA* = 3.5 °C, Table 1), whereas Invader probes with modified 3-mer or unmodified 6-mer overhangs are moderately activated (*TA* = 11-13 °C, **ON5**:**ON6** and **ON7**:**ON8**, Table 1). Invader probe **ON9**:**ON10**, which features modified 6-mer overhangs, is strongly activated for dsDNA-recognition (*TA* = 30 °C, Table 1). This is the result of a highly destabilized probe duplex (ΔT_m = -23 °C, Table 1) and moderately stabilized probe-target duplexes (ΔT_m = 3.5 °C each, Table 1) as compared to the 33-mer dsDNA target. The impact of the +1 interstrand zipper arrangements of 2'-*O*-(pyren-1-yl)methyl-RNA monomers (i.e., energetic hotspots) in activating Invader probes for dsDNA-recognition is underscored by the markedly lower *TA* value for control probe **ON11**:**ON12** which lacks the energetic hotspots (*TA* = 6.5 °C, Table 1). Along similar lines, **ON13**:**ON14**, which lacks hotspots and features unmodified overhangs, is not activated for dsDNA-recognition (*TA* = -1.5 °C, Table 1). Conventional 19-mer Invader probes **ON15**:**ON10** and **ON9**:**ON16** are only moderately activated for DNA recognition (*TA* ~ 14 °C, Table 1), in large part due to the high probe stability.

Enthalpic and entropic parameters associated with formation of double-stranded probes and duplexes between individual probe strands and DNA1 or DNA2. Formation of the double-stranded probes is less enthalpically favorable than formation of **DNA1**:**DNA2** (i.e., $\Delta\Delta H$ = 112-321 kJ/mol, Table S2). This is expected for two reasons, i.e., i) the double-stranded regions of the probes have fewer base pairs (bps) than **DNA1**:**DNA2** (i.e., 13 or 19 bps vis-à-vis 33 bps), and ii) the double-stranded regions of all probes – except for **ON11**:**ON12** and **ON13**:**ON14** - feature two or four +1 interstrand zipper arrangements of 2'-*O*-(pyren-1-yl)methyl-RNA monomers, which are known to destabilize duplexes[S3,S4] due to violation of the nearest neighbor exclusion principle.[S5,S6]

Formation of duplexes between short individual probe strands and the corresponding single-stranded 33-mer DNA strands is generally less enthalpically favorable than formation of **DNA1**:**DNA2** (e.g., $\Delta\Delta H$ for **ON2**/**ON4**/**ON6**:**DNA1** = 150-239 kJ/mol, Table S2). Conversely, formation of duplexes between long individual probe strands and the corresponding 33-mer single-stranded DNA target is generally more enthalpically favorable than formation of **DNA1**:**DNA2**, presumably due to the stabilizing effect of intercalating pyrenes[S3,S4] (e.g., $\Delta\Delta H$ for **ON8**/**ON10**/**ON12**/**ON14**/**ON16**:**DNA1** between -228 and -109 kJ/mol, Table S2). Consequently, the calculated change in reaction enthalpy upon probe-mediated recognition of the 33-mer target **DNA1**:**DNA2** is enthalpically unfavorable for short Invader probes (e.g., see ΔH_{rec} for **ON3**:**ON4** and **ON5**:**ON6**, Table S2), but enthalpically favorable for long Invader probes (e.g., ΔH_{rec} for **ON7**:**ON8**/**ON9**:**ON10**/**ON15**:**ON10**/**ON9**:**ON16** between -654 and -236 kJ/mol, Table S2).

Enthalpy-entropy compensation is observed, i.e., whenever formation of a given duplex is enthalpically favorable (Table S2), it is entropically unfavorable (Table S3). Accordingly, the calculated change in reaction entropy upon probe-mediated recognition of the 33-mer target **DNA1**:**DNA2** is entropically favorable for short Invader probes (e.g., see $-T\Delta S^{310}_{rec}$ for **ON3**:**ON4**

and **ON5**:**ON6**, Table S3) and unfavorable for long Invader probes (e.g., $-T\Delta S^{310}_{rec}$ for **ON7**:**ON8**/**ON9**:**ON10** /**ON15**:**ON10**/**ON9**:**ON16** between +220 and +567 kJ/mol, Table S3).

Table S2. Change in enthalpy (ΔH) upon formation of probe duplexes and duplexes between individual probe strands and **DNA1** or **DNA2**. Also shown is the calculated change in reaction enthalpy upon probe-mediated recognition of 33-mer target **DNA1**:**DNA2** (ΔH_{rec}).[a]

Probe	Sequence	ΔH [$\Delta\Delta H$] (kJ/mol)			ΔH_{rec} (kJ/mol)
		probe duplex	5'-probe vs DNA2	3'-probe vs DNA1	
ON1	5'-GGTA**U**A**U**ATAGGC	-406	-564	-368	-8
ON2	3'-CCATA**U**A**U**ATCCG	[+112]	[-46]	[+150]	
ON3	5'-ACA-GGTA**U**A**U**ATAGGC	-270	-264	-279	+245
ON4	3'-CCATA**U**A**U**ATCCG-GCG	[+248]	[+254]	[+239]	
ON5	5'-A**C**A-GGTA**U**A**U**ATAGGC	-261	-360	-299	+120
ON6	3'-CCATA**U**A**U**ATCCG-G**C**G	[+257]	[+158]	[+219]	
ON7	5'-TGCACA-GGTA**U**A**U**ATAGGC	-277	-361	-670	-236
ON8	3'-CCATA**U**A**U**ATCCG-GCGTAT	[+241]	[+157]	[-152]	
ON9	5'-**U**GCA**C**A-GGTA**U**A**U**ATAGGC	-197	-718	-647	-650
ON10	3'-CCATA**U**A**U**ATCCG-G**C**GTA**U**	[+321]	[-200]	[-129]	
ON11	5'-**U**GCA**C**A-GGTATATATAGGC	-259	-506	-627	-356
ON12	3'-CCATATATATCCG-G**C**GTA**U**	[+259]	[+12]	[-109]	
ON13	5'-TGCACA-GGTATATATAGGC	-523	-639	-629	-227
ON14	3'-CCATATATATCCG-GCGTAT	[-5]	[-121]	[-111]	
ON15	5'-GGTA**U**A**U**ATAGGC-**C**GCA**U**A	-307	-712	-647	-534
ON10	3'-CCATA**U**A**U**ATCCG-G**C**GTA**U**	[+211]	[-194]	[-129]	
ON9	5'-**U**GCA**C**A-GGTA**U**A**U**ATAGGC	-364	-718	-746	-582
ON16	3'- A**C**GTG**U**-CCATA**U**A**U**ATCCG	[+154]	[-200]	[-228]	

[a] $\Delta\Delta H$ is calculated relative to the unmodified 33-mer target DNA duplex **DNA1**:**DNA2** (ΔH = -518 kJ/mol). ΔH_{rec} = ΔH (5'-probe:**DNA2**) + ΔH (3'-probe:**DNA1**) - ΔH (probe duplex) - ΔH (**DNA1**:**DNA2**). For experimental conditions, see Table 1.

Table S3. Change in entropy at 310 K ($-T\Delta S^{310}$) upon formation of probe duplexes and duplexes between individual probe strands and **DNA1** or **DNA2**. Also shown is the calculated change in reaction entropy upon probe-mediated recognition of 33-mer target **DNA1**:**DNA2** ($-T\Delta S^{310}_{rec}$).[a]

Probe	Sequence	$-T\Delta S^{310}$ [$\Delta(T\Delta S^{310})$] (kJ/mol)			$-T\Delta S^{310}_{rec}$ (kJ/mol)
		probe duplex	5'-probe vs DNA2	3'-probe vs DNA1	
ON1 **ON2**	5'-GGTA**U**A**U**ATAGGC 3'-CCATA**U**A**U**ATCCG	+357 [-67]	+493 [+69]	+310 [-114]	+22
ON3 **ON4**	5'-ACA-GGTA**U**A**U**ATAGGC 3'-CCATA**U**A**U**ATCCG-GCG	+226 [-198]	+210 [-214]	+218 [-206]	-222
ON5 **ON6**	5'-A**C**A-GGTA**U**A**U**ATAGGC 3'-CCATA**U**A**U**ATCCG-G**C**G	+215 [-209]	+294 [-130]	+235 [-189]	-110
ON7 **ON8**	5'-TGCACA-GGTA**U**A**U**ATAGGC 3'-CCATA**U**A**U**ATCCG-GCGTAT	+229 [-195]	+294 [-130]	+579 [+155]	+220
ON9 **ON10**	5'-**U**GCA**C**A-GGTA**U**A**U**ATAGGC 3'-CCATA**U**A**U**ATCCG-G**C**GTA**U**	+150 [-274]	+599 [+175]	+536 [+112]	+561
ON11 **ON12**	5'-**U**GCA**C**A-GGTATATATAGGC 3'-CCATATATATCCG-G**C**GTA**U**	+207 [-217]	+426 [+2]	+535 [+111]	+330
ON13 **ON14**	5'-TGCACA-GGTATATATAGGC 3'-CCATATATATCCG-GCGTAT	+477 [+53]	+563 [+139]	+554 [+130]	+216
ON15 **ON10**	5'-GGTA**U**A**U**ATAGGC-**C**GCA**U**A 3'-CCATA**U**A**U**ATCCG-G**C**GTA**U**	+243 [-181]	+593 [+169]	+536 [+112]	+462
ON9 **ON16**	5'-**U**GCA**C**A-GGTA**U**A**U**ATAGGC 3'- A**C**GTG**U**-CCATA**U**A**U**ATCCG	+294 [-130]	+599 [+175]	+623 [+199]	+504

[a] $\Delta(T\Delta S^{310})$ is calculated relative to the unmodified 33-mer target DNA duplex **DNA1**:**DNA2** ($-T\Delta S^{310}$ = 424 kJ/mol). $-T\Delta S^{310}_{rec}$= $\Delta(T\Delta S^{310})$ (5'-probe:**DNA2**) + $\Delta(T\Delta S^{310})$ (3'-probe:**DNA1**) - $\Delta(T\Delta S^{310})$ (probe duplex). For experimental conditions, see Table 1.

Table S4. Quantification of **DNA1**:**DNA2**-recognition at 37 °C using a 5-fold molar excess of different double-stranded probes.[a]

Probe	Sequence	% Recognition
1:2	5'-GGTA**U**A**U**ATAGGC-3' 3'-CCATA**U**A**U**ATCCG-5'	<5
3:4	5'-ACA-GGTA**U**A**U**ATAGGC-3' 3'-CCATA**U**A**U**ATCCG-GCG-5'	<5
5:6	5'-A**C**A-GGTA**U**A**U**ATAGGC-3' 3'-CCATA**U**A**U**ATCCG-G**C**G-5'	<5
7:8	5'-TGCACA-GGTA**U**A**U**ATAGGC-3' 3'-CCATA**U**A**U**ATCCG-GCGTAT-5'	30 ± 6
9:10	5'-**U**GCA**C**A-GGTA**U**A**U**ATAGGC-3' 3'-CCATA**U**A**U**ATCCG-G**C**GTA**U**-5'	45 ± 6
11:12	5'-**U**GCA**C**A-GGTATATATAGGC-3' 3'-CCATATATATCCG-G**C**GTA**U**-5'	39 ± 4
13:14	5'-TGCACA-GGTATATATAGGC-3' 3'-CCATATATATCCG-GCGTAT-5'	<5
15:10	5'-GGTA**U**A**U**ATAGGC-**C**GCA**U**A-3' 3'- CCATA**U**A**U**ATCCG-G**C**GTA**U**-5'	<5
9:16	5'-**U**GCA**C**A-GGTA**U**A**U**ATAGGC-3' 3'-A**C**GTG**U**-CCATA**U**A**U**ATCCG-5'	<5
17:18	5'-**t**GCA**c**A-GGTA**U**A**U**ATAGGC-3' 3'-CCATA**U**A**U**ATCCG-G**c**GTA**t**-5'	46 ± 5
19:20	5'-**t**G**c**AC**a**-GG**U**A**U**ATA**U**AGGC-3' 3'-CCA**U**A**U**ATA**U**CCG-**g**CG**t**A**t**-5'	43 ± 6

[a]Experiments were performed in triplicate. Conditions are described in Fig. 2.

Supplemental discussion of dsDNA-targeting properties of ON7:ON8-ON13:ON14. We were initially surprised to observe that **ON7**:**ON8**, **ON11**:**ON12** and – to a lesser extent **ON13**:**ON14** – result in recognition of **DNA1**:**DNA2** given that a net loss of eight base pairs ensues, i.e., the 13 bps of the double-stranded probes and 33 bps of **DNA1**:**DNA2** denature to form two 19-mer probe-target duplexes, each featuring a 4-mer and a 10-mer overhang (Fig. S26 - left). We speculate that i) the 1-3 outermost base pairs at each end of **DNA1**:**DNA2** are subject to end-fraying effects[S7] and thus only contribute minimally to the overall duplex stability, whereas ii) the overhangs in the probe duplexes and probe-target duplexes reduce fraying due to capping effects, such that the actual energy loss upon recognition of **DNA1**:**DNA2** more closely corresponds to a loss of 2-6 bps. We further speculate that this net loss of base pairs is negated using affinity-enhancing modifications and/or an excess of probe.

Analogously, recognition of **DNA1**:**DNA2** by **ON3**:**ON4** or **ON5**:**ON6** would entail a net loss of 14 bps, i.e., the 13 bps of the double-stranded probes and the 33 bps of **DNA1**:**DNA2** being denatured to form two 16-mer duplexes, each encompassing a 7-mer and a 10-mer single-stranded overhang (Fig. S26 - right). Taking end-fraying effects into account, the loss in energy likely corresponds more closely to 8-12 bps, which, in contrast, cannot be negated using an excess of probe and/or by incorporating 2-3 affinity-enhancing modifications in each probe strand.

To test this hypothesis, **ON7**:**ON8**-**ON13**:**ON14** were incubated with an extended version of **DNA1**:**DNA2**, i.e., a 39-mer dsDNA target in which three additional base pairs are added to each end (Fig. S27). Recognition is expected to result in a net loss of 14 bps (and 8-12 bps if end-fraying effects as discussed above are considered). Indeed, recognition of **DNA1**:**DNA2** is not observed with **ON7**:**ON8**, **ON11**:**ON12** or **ON13**:**ON14**, while less efficient recognition

(compared to recognition of **DNA1**:**DNA2**) is observed with **ON9**:**ON10**, thus supporting the hypothesis (Fig. S27).

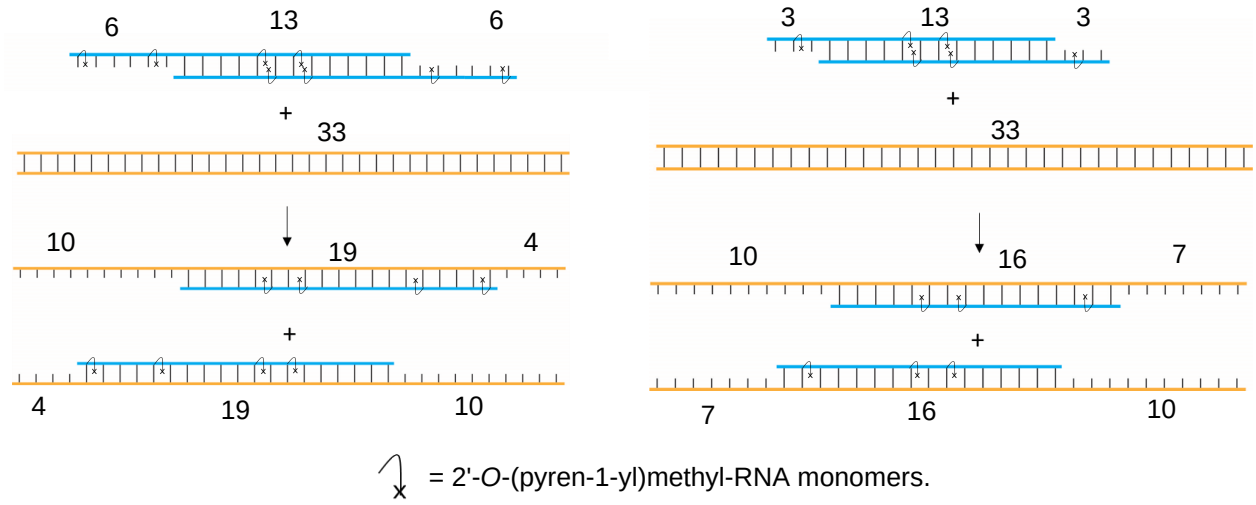

Figure S26. Conceptual illustration of dsDNA-recognition using toehold probes.

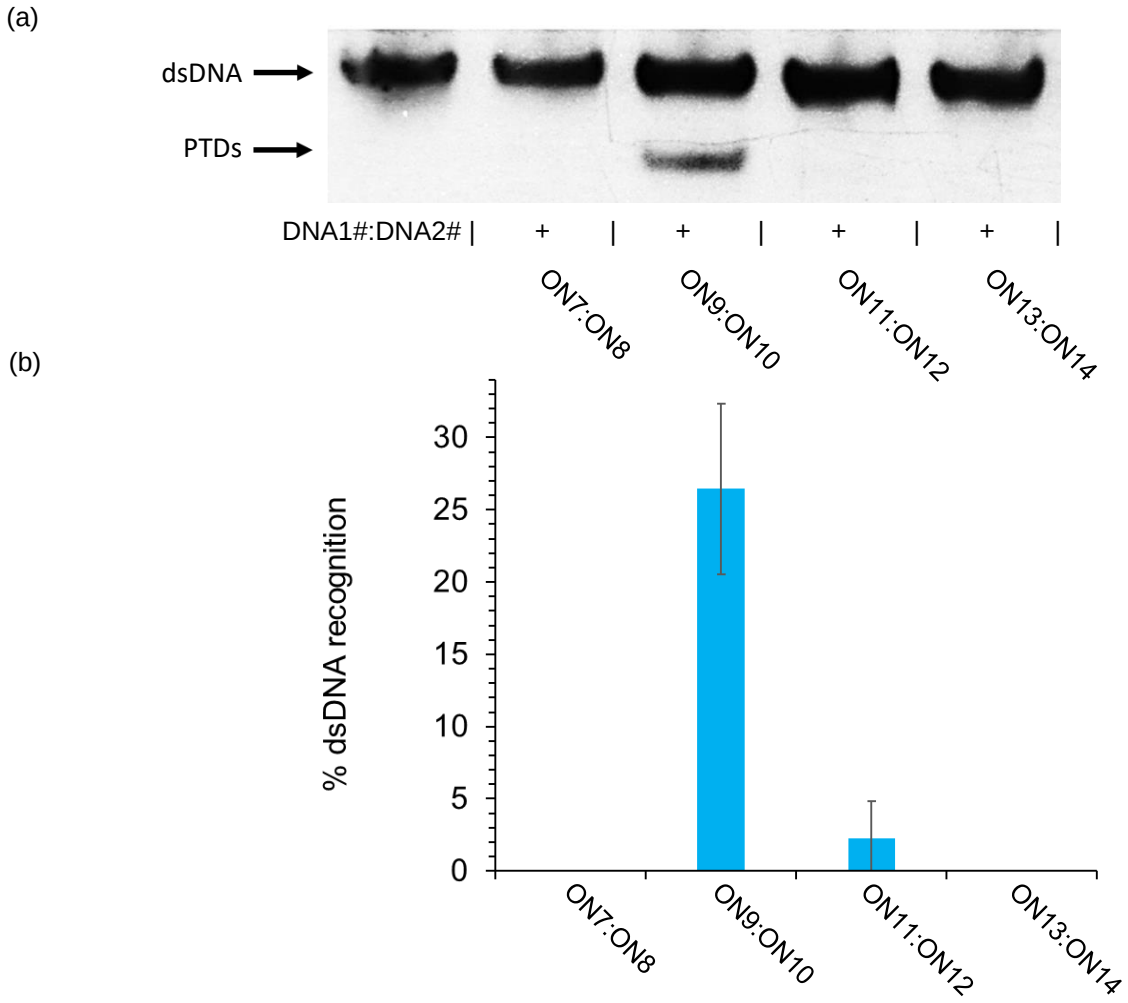

Figure S27. (a) Representative gel electrophoretograms from recognition experiments in which 39-mer dsDNA target **DNA1#**:**DNA2#** was incubated with a 5-fold molar excess of various probes. **DNA1#** = 5'-TCA AAG CTG CAC AGG TAT ATA TAG GCC GCA TAT GCA AGT and **DNA2#** = 3'-AGT TTC GAC GTG TCC ATA TAT ATC CGG CGT ATA CGT TCA. PTD = probe-target duplex. (b) Histogram depicting averaged results from at least three independent recognition experiments with error bars representing standard deviation. Conditions: 3'-DIG-labeled **DNA1#**:**DNA2#** (50 nM) was incubated with a 5-fold molar excess of the specified probe in HEPES buffer (50 mM HEPES, 100 mM NaCl, 5 mM $MgCl_2$, pH 7.2, 10% sucrose, 1.44 mM spermine tetrahydrochloride) for 17 h at 37 °C.

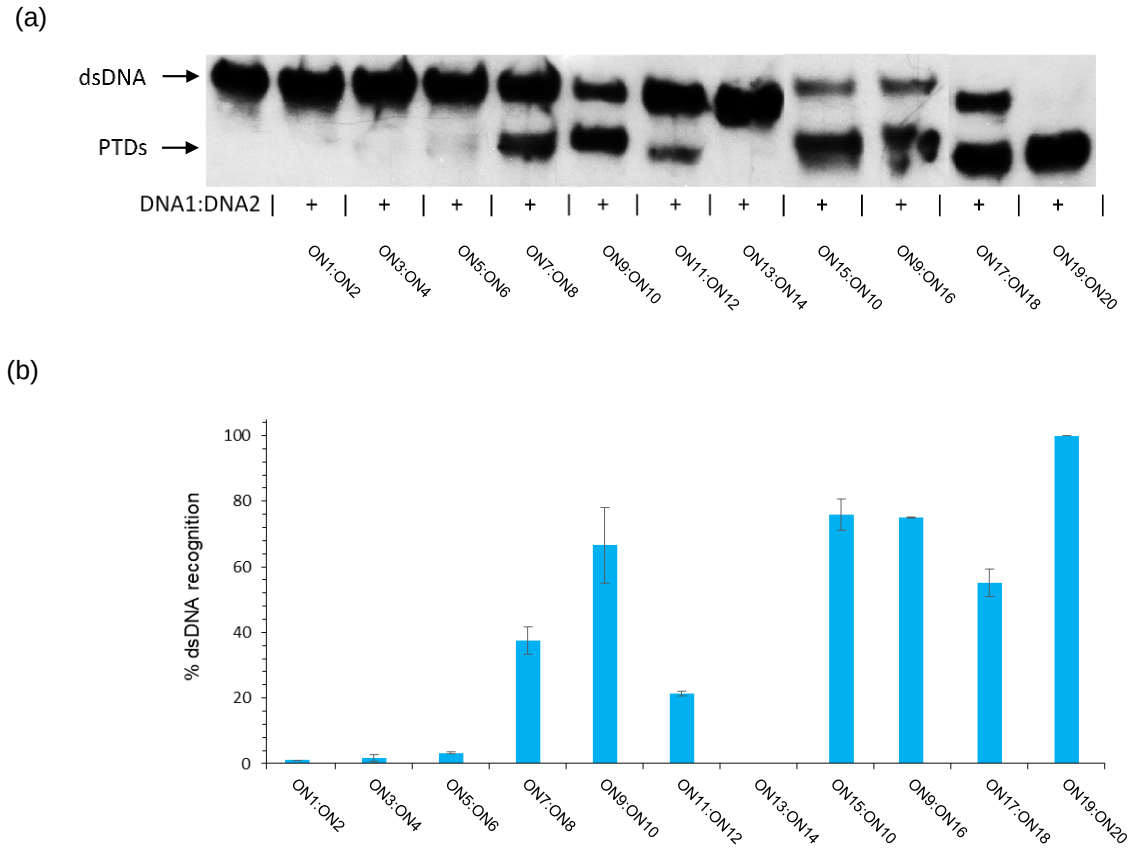

Figure S28. (a) Representative gel electrophoretograms from experiments in which **DNA1**:**DNA2** was incubated with different Invader probes under heat-shock conditions. PTD = probe-target duplexes. (b) Histogram depicting averaged results from at least three independent recognition experiments with error bars representing standard deviation. DIG-labeled 33-mer target **DNA1**:**DNA2** (50 nM) was mixed with a 5-fold molar excess of different double-stranded probes in HEPES buffer (100 mM NaCl, 5 mM $MgCl_2$, 10% sucrose, 1.4 mM spermine tetrahydrochloride, pH 7.2), briefly heated (3 min, 90 °C), then cooled to 37 °C and incubated at 37 °C for 17 h. Results are tabulated in Table S5.

Table S5. Quantification of **DNA1**:**DNA2**-recognition using a 5-fold molar excess of various double-stranded probes under heat-shock conditions.[a]

Probe	Sequence	% Recognition
1:2	5'-GGTA**U**A**U**ATAGGC-3' 3'-CCATA**U**A**U**ATCCG-5'	<5
3:4	5'-ACA-GGTA**U**A**U**ATAGGC-3' 3'-CCATA**U**A**U**ATCCG-GCG-5'	<5
5:6	5'-A**C**A-GGTA**U**A**U**ATAGGC-3' 3'-CCATA**U**A**U**ATCCG-G**C**G-5'	<5
7:8	5'-TGCACA-GGTA**U**A**U**ATAGGC-3' 3'-CCATA**U**A**U**ATCCG-GCGTAT-5'	38 ± 4
9:10	5'-**U**GCA**C**A-GGTA**U**A**U**ATAGGC-3' 3'-CCATA**U**A**U**ATCCG-G**C**GTA**U**-5'	67 ± 4
11:12	5'-**U**GCA**C**A-GGTATATATAGGC-3' 3'-CCATATATATCCG-G**C**GTA**U**-5'	22± 1
13:14	5'-TGCACA-GGTATATATAGGC-3' 3'-CCATATATATCCG-GCGTAT-5'	<5
15:10	5'-GGTA**U**A**U**ATAGGC-**C**GCA**U**A-3' 3'- CCATA**U**A**U**ATCCG-G**C**GTA**U**-5'	76± 5
9:16	5'-**U**GCA**C**A-GGTA**U**A**U**ATAGGC-3' 3'-A**C**GTG**U**-CCATA**U**A**U**ATCCG-5'	75± 1
17:18	5'-**t**GCA**c**A-GGTA**U**A**U**ATAGGC-3' 3'-CCATA**U**A**U**ATCCG-G**c**GTA**t**-5'	55 ± 4
19:20	5'-**t**G**c**AC**a**-GG**U**A**U**ATA**U**AGGC-3' 3'-CCA**U**A**U**ATA**U**CCG-**g**CG**t**A**t**-5'	100

[a]Experiments were performed in triplicate. Conditions are described in Fig. S28.

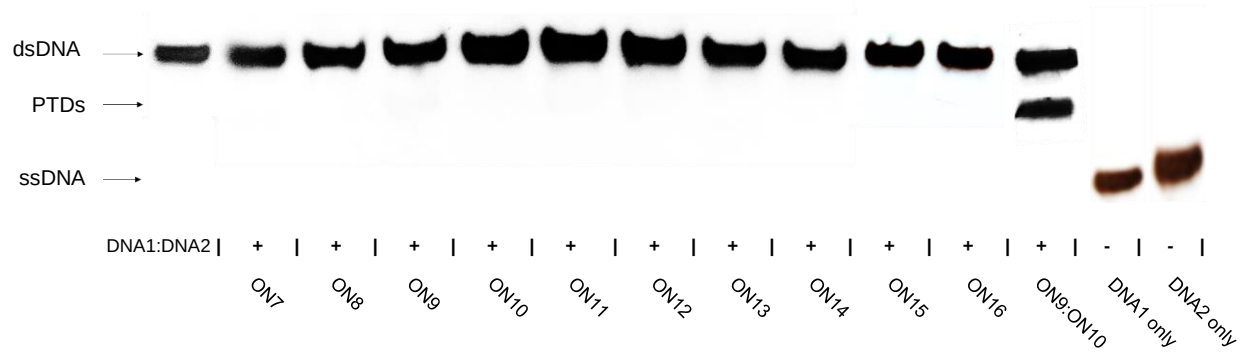

Figure S29. Representative gel electrophoretograms from recognition experiments in which **DNA1**:**DNA2** (dsDNA, 50 nM) was incubated with a 5-fold molar excess of individual probe strands **ON7**-**ON16** at 37 °C. Experimental conditions are as described in Fig. 2. PTD = probe-target duplex.

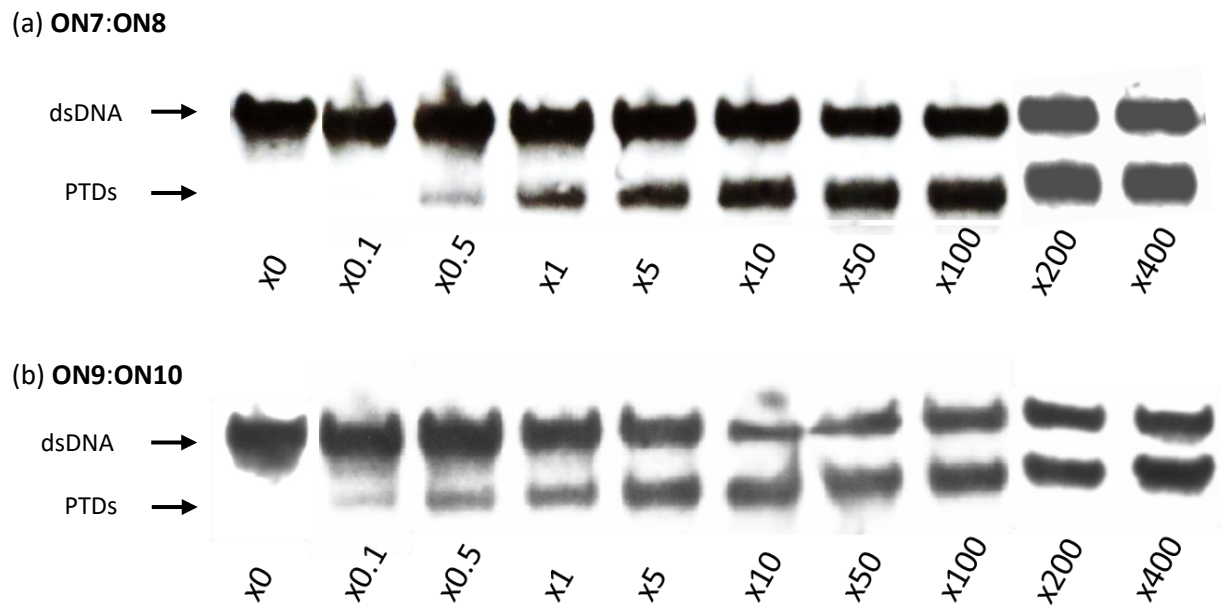

Figure S30. Representative electrophoretograms from dose-response experiments in which **DNA1**:**DNA2** (50 nM) was incubated with a variable excess of a) **ON7**:**ON8** or b) **ON9**:**ON10** at 37 °C. Experimental conditions are as described in Fig. 2.

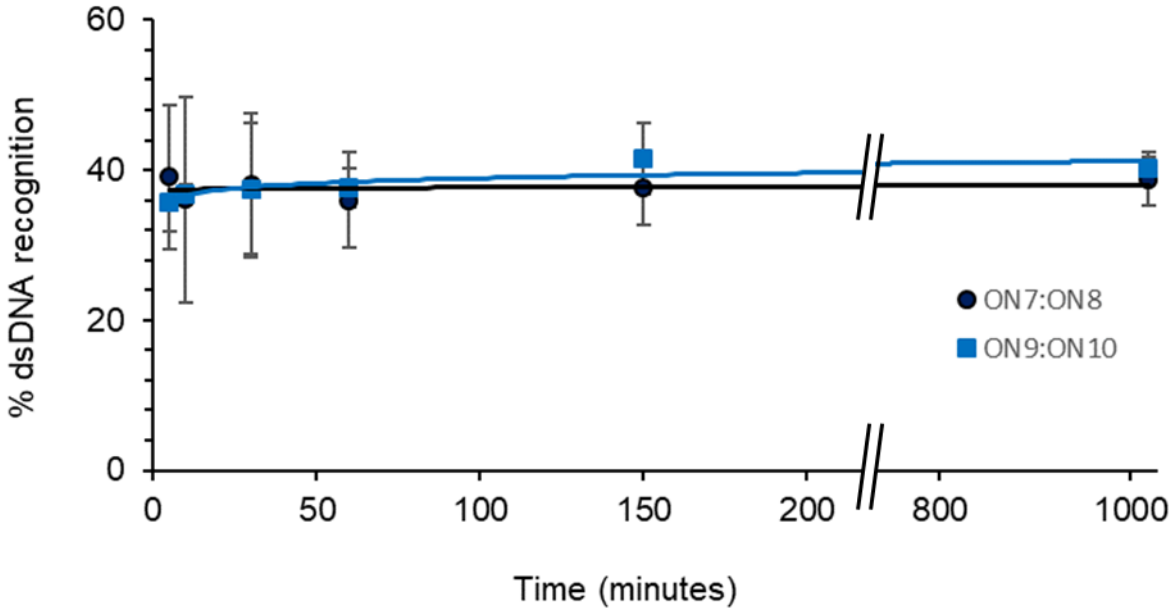

Figure S31. Time-course experiments in which **DNA1**:**DNA2** (50 nM) was incubated with a 5-fold excess of toehold Invader probes **ON7**:**ON8** or **ON9**:**ON10** at 37 °C in HEPES buffer (100 mM NaCl, 5 mM $MgCl_2$, 10% sucrose, 1.44 mM spermine tetrahydrochloride, pH 7.2). Aliquots were taken at the specified time-points, flash-frozen and stored in liquid N_2 until electrophoresis was performed as described in Fig. 2.

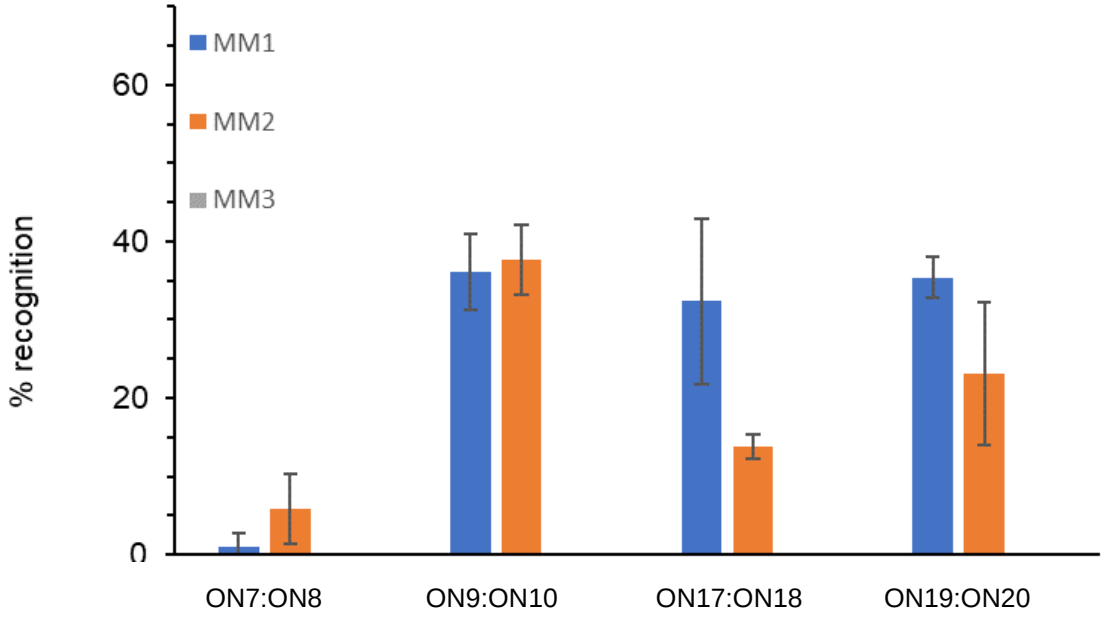

Figure S32. Histogram depicting averaged results from at least three experiments in which pre-annealed 3'-DIG-labelled **MM1**-**MM3** were incubated with a 5-fold molar excess of various pre-annealed Invader probes at 37 °C for 17 h in HEPES buffer as outlined in Fig. 2. Error bars represent standard deviation. For representative electrophoretograms, see Figs. 4 and 5. Sequences of **MM1**-**MM3** are shown in Table S6.

Table S6. Thermal denaturation temperatures (T_ms) of **MM1**-**MM3**, as well as duplexes between individual probe strands **ON7** or **ON8** and the corresponding mismatched DNA strands. *TA* values for recognition of **MM1**-**MM3** by **ON7**:**ON8** are also shown.[a]

DNA	Sequence	T_m (°C)			
		dsDNA	5'-DNA vs ON8	3'-DNA vs ON7	*TA* (°C)
DNA1	5'-AAGCTG CAC AGG TAT ATA TAG GCC GCA TATGCA-3'	72.0	67.0	60.0	11.0
DNA2	3'-TTCGAC GTG TCC ATA TAT ATC CGG CGT ATACGT-5'				
DNA3	5'-AAGCTG CAC AGG TAT TTA TAG GCC GCA TATGCA-3'	74.0	64.5	57.5	4.0
DNA4	3'-TTCGAC GTG TCC ATA AAT ATC CGG CGT ATACGT-5'				
DNA5	5'-AAGCTG GAC AGG TAT ATA TAG GCC GCT TATGCA-3'	72.0	66.0	58.0	8.0
DNA6	3'-TTCGAC CTG TCC ATA TAT ATC CGG CGA ATACGT-5'				
DNA7	5'-AAGCTG GAC AGG TAT TTA TAG GCC GCT TATGCA-3'	72.5	62.5	49.0	-5.0
DNA8	3'-TTCGAC CTG TCC ATA AAT ATC CGG CGA ATACGT-5'				

[a] Position of mismatched base pairs relative to **ON7**:**ON8** highlighted in yellow. *TA* is calculated for **ON7**:**ON8** (T_m = 44.0 °C). Experimental conditions are as described in Table 1. For a definition of *TA*, see the main manuscript. **MM1** = **DNA3**:**DNA4**, **MM2** = **DNA5**:**DNA6**, and **MM3** = **DNA7**:**DNA8**. For the corresponding thermal denaturation curves, see Fig S23.

Table S7. Thermal denaturation temperatures (T_ms) of **MM1**-**MM3**, as well as, duplexes between individual probe strands **ON9** or **ON10** and the corresponding mismatched DNA strands. *TA* values for recognition of **MM1**-**MM3** by **ON9**:**ON10** are also shown.[a]

DNA	Sequence	T_m (°C)			
		dsDNA	5'-DNA vs ON10	3'-DNA vs ON9	*TA* (°C)
DNA1	5'-AAGCTG CAC AGG TAT ATA TAG GCC GCA TATGCA-3'	72.0	75.5	75.5	30.0
DNA2	3'-TTCGAC GTG TCC ATA TAT ATC CGG CGT ATACGT-5'				
DNA3	5'-AAGCTG CAC AGG TAT TTA TAG GCC GCA TATGCA-3'	74.0	72.0	67.5	16.5
DNA4	3'-TTCGAC GTG TCC ATA AAT ATC CGG CGT ATACGT-5'				
DNA5	5'-AAGCTG GAC AGG TAT ATA TAG GCC GCT TATGCA-3'	72.0	72.0	68.0	19.0
DNA6	3'-TTCGAC CTG TCC ATA TAT ATC CGG CGA ATACGT-5'				
DNA7	5'-AAGCTG GAC AGG TAT TTA TAG GCC GCT TATGCA-3'	72.5	72.0	59.0	9.5
DNA8	3'-TTCGAC CTG TCC ATA AAT ATC CGG CGA ATACGT-5'				

[a] Position of mismatched base pairs relative to probe highlighted in yellow. *TA* is calculated for **ON9**:**ON10** (T_m = 49.0 °C). Experimental conditions are as described in Table 1. For a definition of *TA*, see the main manuscript. **MM1** = **DNA3**:**DNA4**, **MM2** = **DNA5**:**DNA6**, and **MM3** = **DNA7**:**DNA8**. For the corresponding thermal denaturation curves, see Fig. S23.

*Additional discussion of enthalpic and entropic parameters observed for **ON17**:**ON18**.* The favorable $\Delta G^{310}_{\mathrm{rec}}$ value for recognition of **DNA1**:**DNA2** using probe **ON17**:**ON18** (Table 2) is a consequence of a highly favorable change in enthalpy (ΔH_{rec} = -342 kJ/mol), Table S8), which only is partially offset by an unfavorable change in entropy ($-T\Delta S^{310}_{rec}$ +279 kJ/mol, Table S9).

Table S8. Change in enthalpy (ΔH) upon formation of probe duplexes and duplexes between individual probe strands and **DNA1** or **DNA2**. The calculated change in reaction enthalpy upon probe-mediated recognition of 33-mer target **DNA1**:**DNA2** (ΔH_{rec}) is also shown.[a]

		ΔH [$\Delta\Delta H$] (kJ/mol)			
Probe	**Sequence**	**probe duplex**	**5'-probe vs DNA2**	**3'-probe vs DNA1**	**ΔH_{rec} (kJ/mol)**
ON17	5'-**t**GCA**c**A-GGTA**U**A**U**ATAGGC	-394	-608	-646	-342
ON18	3'-CCATA**U**A**U**ATCCG-G**c**GTA**t**	[+124]	[-90]	[-128]	
ON19	5'-**t**G**c**AC**a**-GG**U**A**U**ATA**U**AGGC	-[b]	-743	-524	nd
ON20	3'-CCA**U**A**U**ATA**U**CCG-**g**CG**t**A**t**		[-225]	[-6]	

[a] $\Delta\Delta H$ is calculated relative to the unmodified 33-mer target DNA duplex **DNA1**:**DNA2** (ΔH = -518 kJ/mol). ΔH_{rec} = ΔH (5'-probe:**DNA2**) + ΔH (3'-probe:**DNA1**) - ΔH (probe duplex) - ΔH (**DNA1**:**DNA2**). For experimental conditions, see Table 1.

Table S9. Change in entropy at 310 K ($-T\Delta S^{310}$) upon formation of probe duplexes and duplexes between individual probe strands and **DNA1** or **DNA2**. The calculated change in reaction entropy upon probe-mediated recognition of 33-mer target **DNA1**:**DNA2** ($-T\Delta S^{310}_{rec}$) is also shown.[a]

		$-T\Delta S^{310}$ [$\Delta(T\Delta S^{310})$] (kJ/mol)			
Probe	**Sequence**	**probe duplex**	**5'-probe vs DNA2**	**3'-probe vs DNA1**	**$-T\Delta S^{310}_{rec}$ (kJ/mol)**
ON17	5'-**t**GCA**c**A-GGTA**U**A**U**ATAGGC	+339	+504	+538	+279
ON18	3'-CCATA**U**A**U**ATCCG-G**c**GTA**t**	[-85]	[+80]	[+114]	
ON19	5'-**t**G**c**AC**a**-GG**U**A**U**ATA**U**AGGC	-[b]	+620	+420	nd
ON20	3'-CCA**U**A**U**ATA**U**CCG-**g**CG**t**A**t**		[+196]	[-4]	

[a] $\Delta(T\Delta S^{310})$ is calculated relative to the unmodified 33-mer target DNA duplex **DNA1**:**DNA2** ($-T\Delta S^{310}$ = 424 kJ/mol). $-T\Delta S^{310}_{rec}$= $\Delta(T\Delta S^{310})$ (5'-probe:**DNA2**) + $\Delta(T\Delta S^{310})$ (3'-probe:**DNA1**) - $\Delta(T\Delta S^{310})$ (probe duplex). For experimental conditions, see Table 1.

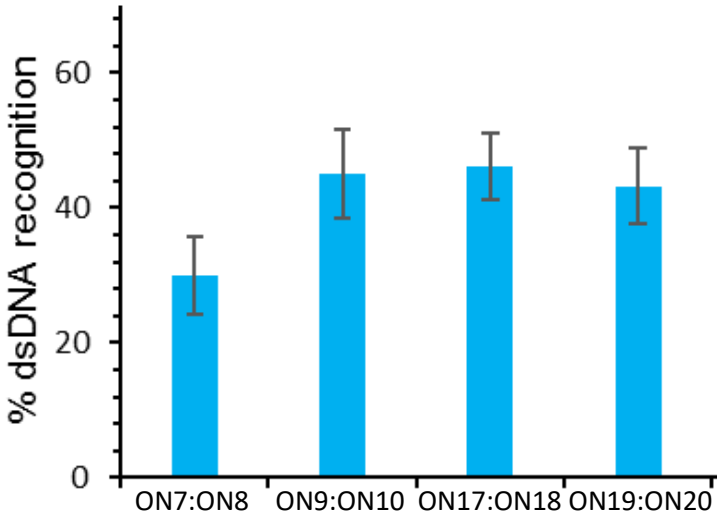

Figure S33. Quantification of at least three independent recognition experiments using model dsDNA target **DNA1**:**DNA2** (50 nM) and a 5-fold molar excess of various Invader probes. Error bars represent standard deviation. Experimental conditions are as outlined in Fig. 2.

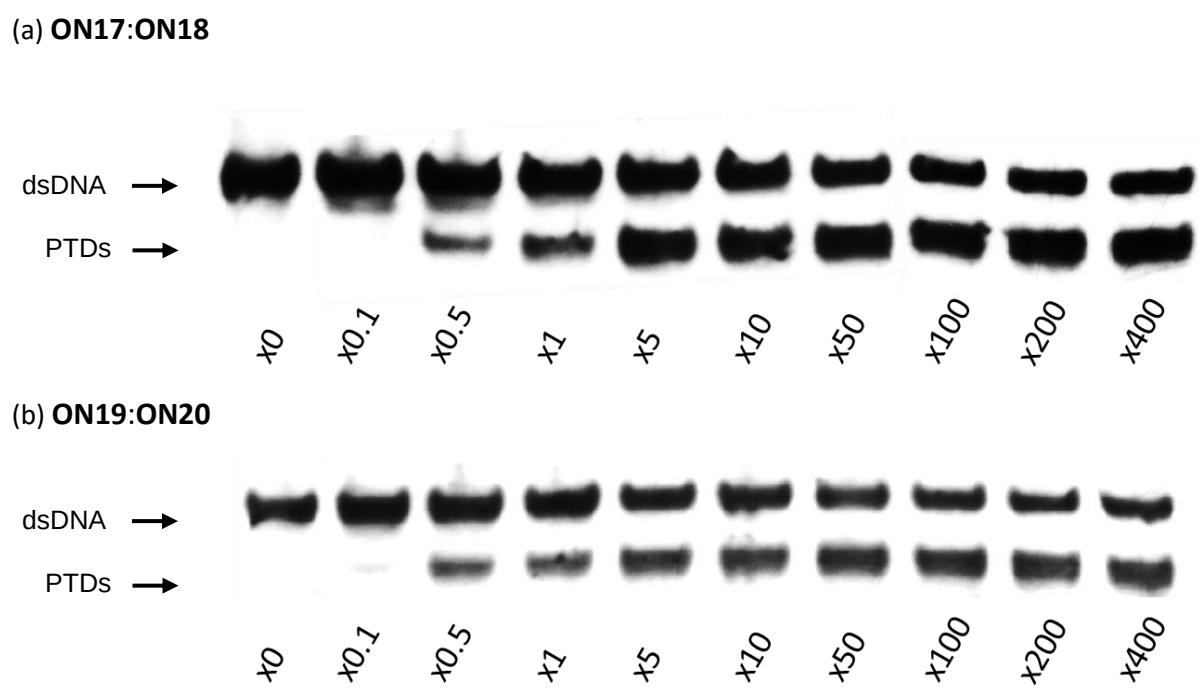

Figure S34. Representative electrophoretograms from experiments in which **DNA1**:**DNA2** (50 nM) was incubated with a variable excess of LNA-modified toehold Invader probes: a) **ON17**:**ON18** and b) **ON19**:**ON20**. Experimental conditions are as described in Fig. 2.

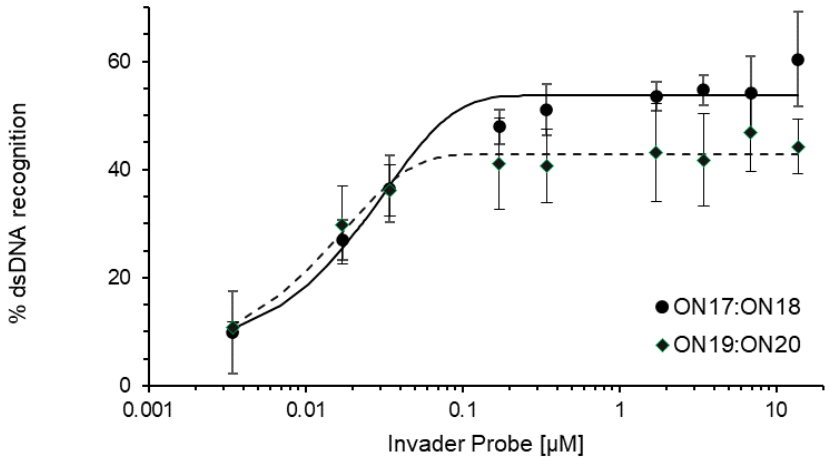

Figure S35. Dose-response curves for recognition of **DNA1**:**DNA2** by LNA-modified Invader probes **ON17**:**ON18** or **ON19**:**ON20**. Curves are constructed based on the electrophoretograms shown in Fig. S34. Experimental conditions are as in Fig. 2.

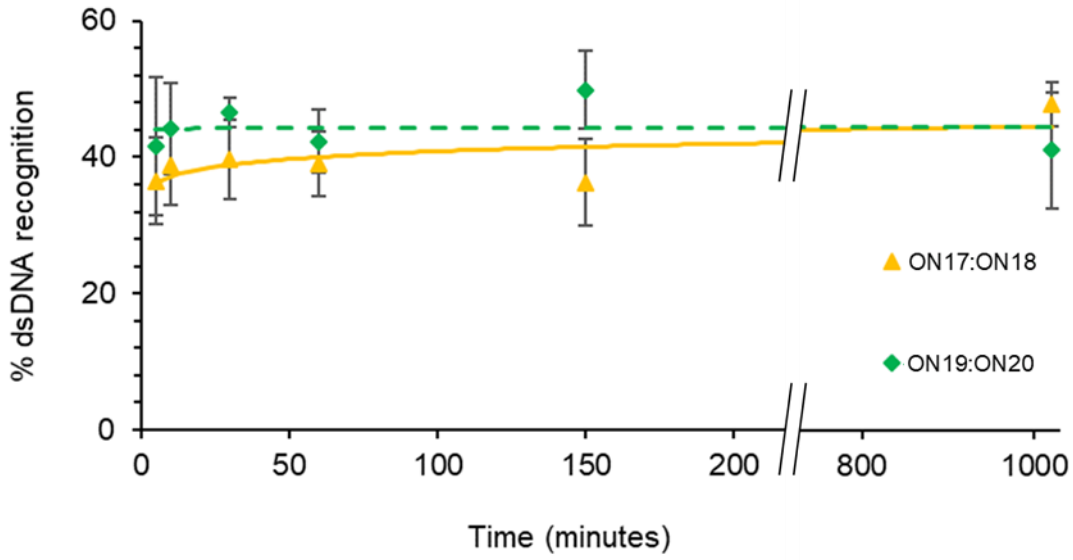

Figure S36. Time-course for recognition of **DNA1**:**DNA2** using LNA-modified toehold Invader probes. **DNA1**:**DNA2** (50 nM) was incubated with 5-fold molar excess of **ON17**:**ON18** or **ON19**:**ON20** at 37 °C in HEPES buffer (100 mM NaCl, 5 mM $MgCl_2$, 10% sucrose, 1.44 mM spermine tetrahydrochloride, pH 7.2). Aliquots were taken at the specified time-points, flash-frozen, and stored in liquid N_2 until being resolved by gel electrophoresis as described in Fig. 2.

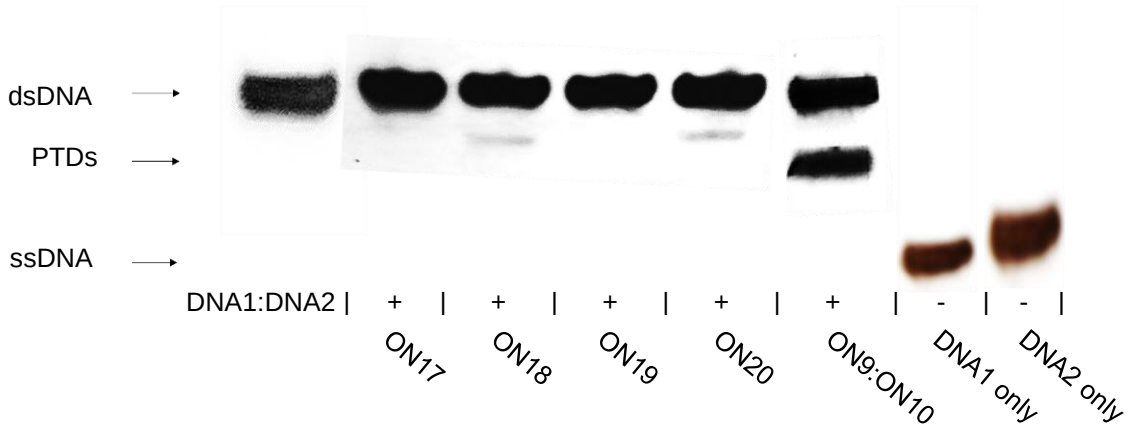

Figure S37. Representative gel eletrophoretograms from recognition experiments in which a 5-fold molar excess of single-stranded probes **ON17**-**ON20** was incubated with **DNA1**:**DNA2**. Experimental conditions are as described in Fig. 2. PTDs = probe-target duplexes.

Table S10. Thermal denaturation temperatures (T_ms) of **MM1**-**MM3** as well as duplexes between individual probe strands **ON17** or **ON18** and the corresponding mismatched DNA strands. *TA* values for recognition of **MM1**-**MM3** by **ON17**:**ON18** are also shown.[a]

DNA	Sequence	T_m (°C)			
		dsDNA	5'-DNA vs ON18	3'-DNA vs ON17	*TA* (°C)
DNA1 **DNA2**	5'-AAG CTG CAC AGG TAT ATA TAG GCC GCA TAT GCA -3' 3'-TTC GAC GTG TC**C** ATA TAT ATC CGG CGT ATA CGT -5'	72.0	73.0	71.5	25.0
DNA3 **DNA4**	5'-AAG CTG CAC AGG TAT TTA TAG GCC GCA TAT GCA -3' 3'-TTC GAC GTG TC**C** ATA AAT ATC CGG CGT ATA CGT -5'	74.0	70.0	66.0	14.5
DNA5 **DNA6**	5'-AAG CTG GAC AGG TAT ATA TAG GCC GCT TAT GCA -3' 3'-TTC GAC CTG TC**C** ATA TAT ATC CGG CGA ATA CGT -5'	72.0	71.5	65.0	17.0
DNA7 **DNA8**	5'-AAG CTG GAC AGG TAT TTA TAG GCC GCT TAT GCA -3' 3'-TTC GAC CTG TC**C** ATA AAT ATC CGG CGA ATA CGT -5'	72.5	68.5	56.0	4.5

[a] Position of mismatched base pairs relative to probe highlighted in yellow. *TA* values are calculated relative to **ON17**:**ON18** (T_m = 47.5 °C). Experimental conditions are as described in Table 1. For a definition of *TA*, see the main manuscript. **MM1** = **DNA3**:**DNA4**, **MM2** = **DNA5**:**DNA6**, and **MM3** = **DNA7**:**DNA8**. For representative denaturation curves, see Fig. S24.

Table S11. Thermal denaturation temperatures (T_ms) of **MM1**-**MM3** as well as duplexes between individual probe strands **ON19** or **ON20** and the corresponding mismatched DNA strands.[a]

DNA	Sequence	T_m (°C)		
		dsDNA	5'-DNA vs ON20	3'-DNA vs ON19
DNA1 **DNA2**	5'-AAG CTG CAC AGG TAT ATA TAG GCC GCA TAT GCA -3' 3'-TTC GAC GTG TC**C** ATA TAT ATC CGG CGT ATA CGT -5'	72.0	79.5	78.0
DNA3 **DNA4**	5'-AAG CTG CAC AGG TAT TTA TAG GCC GCA TAT GCA -3' 3'-TTC GAC GTG TC**C** ATA AAT ATC CGG CGT ATA CGT -5'	74.0	76.5	71.0
DNA5 **DNA6**	5'-AAG CTG GAC AGG TAT ATA TAG GCC GCT TAT GCA -3' 3'-TTC GAC CTG TC**C** ATA TAT ATC CGG CGA ATA CGT -5'	72.0	76.5	68.5
DNA7 **DNA8**	5'-AAG CTG GAC AGG TAT TTA TAG GCC GCT TAT GCA -3' 3'-TTC GAC CTG TC**C** ATA AAT ATC CGG CGA ATA CGT -5'	72.5	73.5	59.5

[a] Position of mismatched base pairs relative to probe highlighted in yellow. Experimental conditions are as described in Table 1. *TA* values could not be calculated since **ON19**:**ON20** did not display a transition. **MM1** = **DNA3**:**DNA4**, **MM2** = **DNA5**:**DNA6**, and **MM3** = **DNA7**:**DNA8**. For representative denaturation curves, see Fig. S24.

Table S12. Sequence and T_m of DNA hairpin **DH1** used in this study.[a]

DNA target	sequence	T_m (°C)
DH1	5′- AAG CTG CAC AGG TAT ATA TAG GCC GCA TAT GCA 3′- TTC GAC GTG TCC ATA TAT ATC CGG CGT ATA CGT $(T)_{10}$	81

[a] Experimental conditions are as stated in Table 1. Representative thermal denaturation curves are shown in Fig. S38.

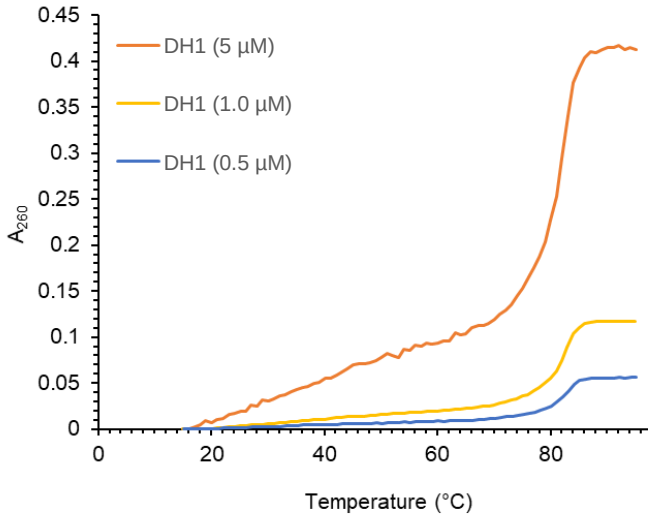

Figure S38. Representative thermal denaturation profiles of 33-mer dsDNA hairpin **DH1** recorded in medium salt buffer at strand concentrations of 0.5 µM, 1.0 µM and 5 µM. The observation of near-identical concentration-independent T_m values suggests that an intramolecular unimolecular hairpin structure is formed. Experimental conditions are as described in Table 1.

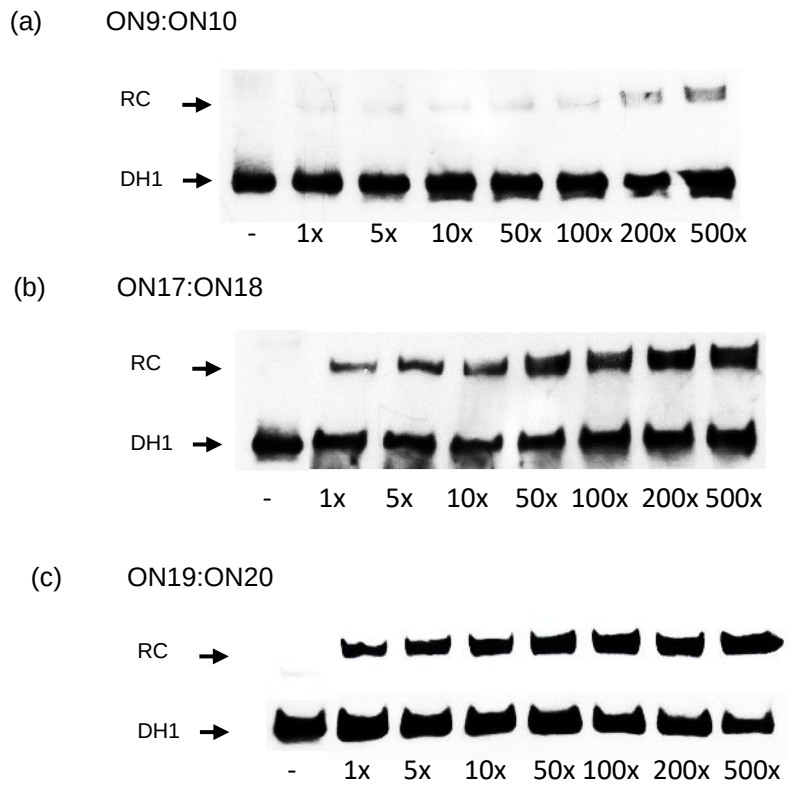

Figure S39. Representative electrophoretograms from recognition experiments in which **DH1** (50 nM) was incubated with a variable excess of a) **ON9**:**ON10**, b) **ON17**:**ON18** or c) **ON19**:**ON20.** Experimental conditions are as described in Fig. 2.

Table S13. Sequences of probes used in FISH experiments, as well as T_ms of probe duplexes and duplexes between individual probe strands and DNA targets.[a]

Probe	Sequence	T_m [ΔT_m] (°C)			
		probe duplex	5'-probe vs DNA10	3'-probe vs DNA9	*TA* (°C)
DYZ-OPTu **DYZ-OPTd**	5'-Cy3-T**g**T**g**TG-T**U**A**U**ATGCTG**U**TCTC-3' 3'-AA**U**A**U**ACGACA**A**GAG-TC**g**G**g**A-Cy3-5'	nt	66.0 [0.0]	69.0 [+3.0]	nd
DYZ-REFu **DYZ-REFd**	5'-Cy3-T**U**A **U**AT GCT G**U**T CTC-3' 3'- AA**U** A**U**A CGA CA**A** GAG-Cy3-5'	56.0[b]	61.0[b]	68.0[b]	+7.0

[a] ΔT_m is calculated relative to the unmodified **DNA9**:**DNA10** duplex (T_m = 66.0 °C). For the sequence of **DNA9**:**DNA10**, see Table S14. Conditions are as described in Table 1.

[b] Values are based on a single measurement, due to limited probe access.

nd = not determinable; nt = no transition

Table S14. Thermal denaturation temperatures (T_ms) of complementary **DNA9**:**DNA10** and non-complementary target **DNA11**:**DNA12**, as well as duplexes between individual DNA strands and individual probe strands.[a]

DNA	Sequence	T_m (°C)		
		dsDNA	5'-DNA: DYZ-OPTd	3'-DNA: DYZ-OPTu
DNA9 **DNA10**	5'-TGAC *TGT GTG TTA TAT GCT GTT CTC AGC CCT* TGAC 3'-ACTG *ACA CAC AAT ATA CGA CAA GAG TCG GGA* ACTG	66.0	69.0	66.0
DNA11 **DNA12**	5'-TGAC *TGT GTC TTA TAT GGT GTT CTC TGC CCT* TGAC 3'-ACTG *ACA CAG AAT ATA CCA CAA GAG ACG GGA* ACTG	66.0	56.0	51.0

[a] Conditions are as described in Table 1. The 27-mer mixed-sequence target region within **DNA9**:**DNA10** is italicized. Positions highlighted in yellow denote the position of mismatched base pairs relative to **DYZ-OPTu**:**DYZ-OPTd**.

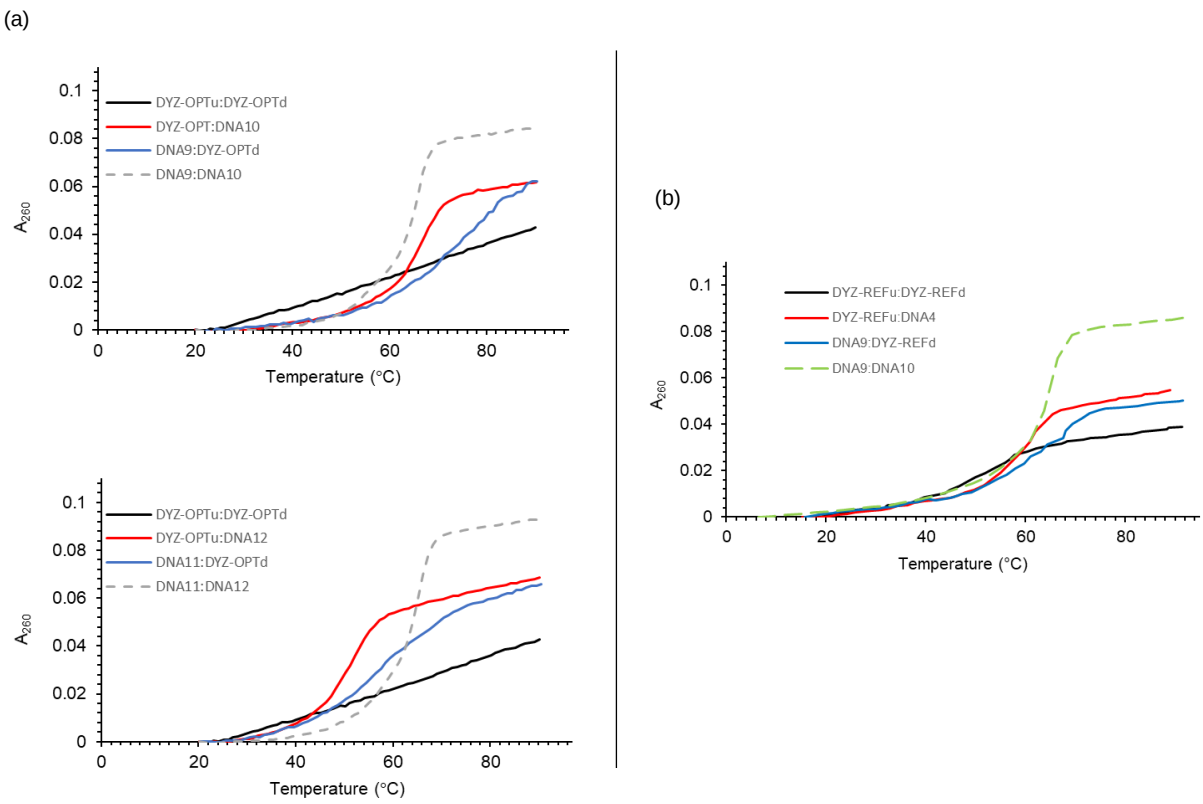

Figure S40. (a) Representative thermal denaturation curves for toehold Invader probe **DYZ-OPT** (**DYZ-OPTu**:**DYZ-OPTd**), duplexes between individual probe strands and single-stranded (non-)complementary DNA targets, as well as **DNA9**:**DNA10** and **DNA11**:**DNA12** (the latter of which differs in sequence at three positions relative to **DNA9**:**DNA10**). (b) Representative thermal denaturation curves for toehold Invader probe **DYZ-REFu**:**DYZ-REFd**, and duplexes between individual probe strands and single-stranded complementary DNA targets, **DNA9**:**DNA10**. For sequences see Table S14. Conditions are as outlined in Table 1.

Table S15. Illustration of matched or mismatched probe-target duplexes that would ensue upon recognition of complementary target **DNA9**:**DAN10** or triply-mismatched target **DNA11**:**DNA12** using **DYZ-OPT**. Positions highlighted in yellow denote the position of mismatched base pairs.

DNA	Sequence
DYZ-OPTu	5'-Cy3-T**g**T **g**TG-T**U**A **U**AT GCT G**U**T CTC
DNA10	3'-ACTG ACA CAC AAT ATA CGA CAA GAG TCG GGA ACTG
DNA9	5'-TGAC TGT GTG TTA TAT GCT GTT CTC AGC CCT TGAC
DYZ-OPTd	3'-AA**U** A**U**A CGA CA**A** GAG-TC**g** G**g**A-Cy3-5'
DYZ-OPTu	5'-Cy3-T**g**T **g**TG-T**U**A **U**AT GCT G**U**T CTC
DNA12	3'-ACTG ACA CAG AAT ATA CCA CAA GAG ACG GGA ACTG
DNA11	5'-TGAC TGT GTC TTA TAT GGT GTT CTC TGC CCT TGAC
DYZ-OPTd	3'-AA**U** A**U**A CGA CA**A** GAG-TC**g** G**g**A-Cy3-5'

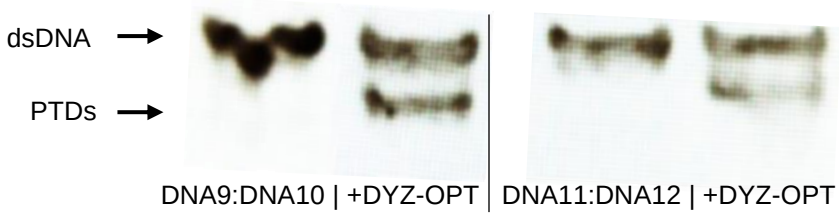

Figure S41. Representative electrophoretograms from experiments in which a 5-fold molar excess of **DYZ-OPT** was incubated with complementary **DNA9**:**DNA10** or non-complementary dsDNA target **DNA11**:**DNA12** (see Table S14 for sequences of **DNA9**:**DNA10**, and **DNA11**:**DNA12**). Pre-annealed 3'-DIG-labeled targets (50 nM) were incubated with pre-annealed Invader probes at 37 °C for 17 h in HEPES buffer as described in Fig. 2.

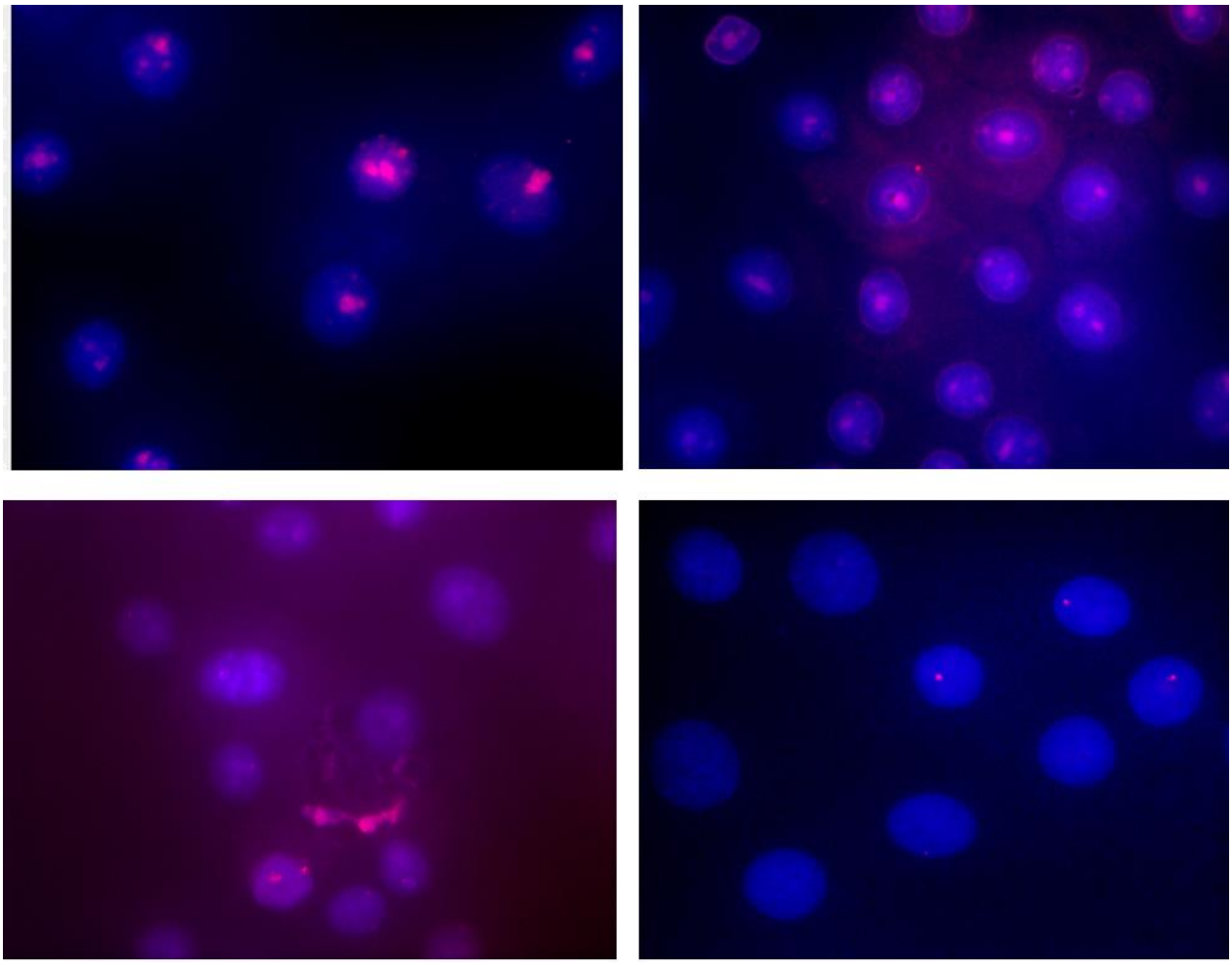

Figure S42. Concentration dependence of **DYZ-OPT**-produced FISH signals under non-denaturing conditions. Images from FISH experiments using fixed male bovine kidney cells and varying quantities of LNA-modified toehold Invader probe **DYZ-OPT**, i.e., 30 ng (top left), 15 ng (top right), 6 ng (bottom left), and 3 ng (bottom right) per 200 µL of 1X PCR buffer. Conditions are otherwise as specified in Fig. 8. Substantial amounts of background signals were observed when using 6-30 ng **DYZ-OPT**. Accordingly, 3 ng of **DYZ-OPT** per 200 µL of 1X PCR buffer was selected as an appropriate concentration.

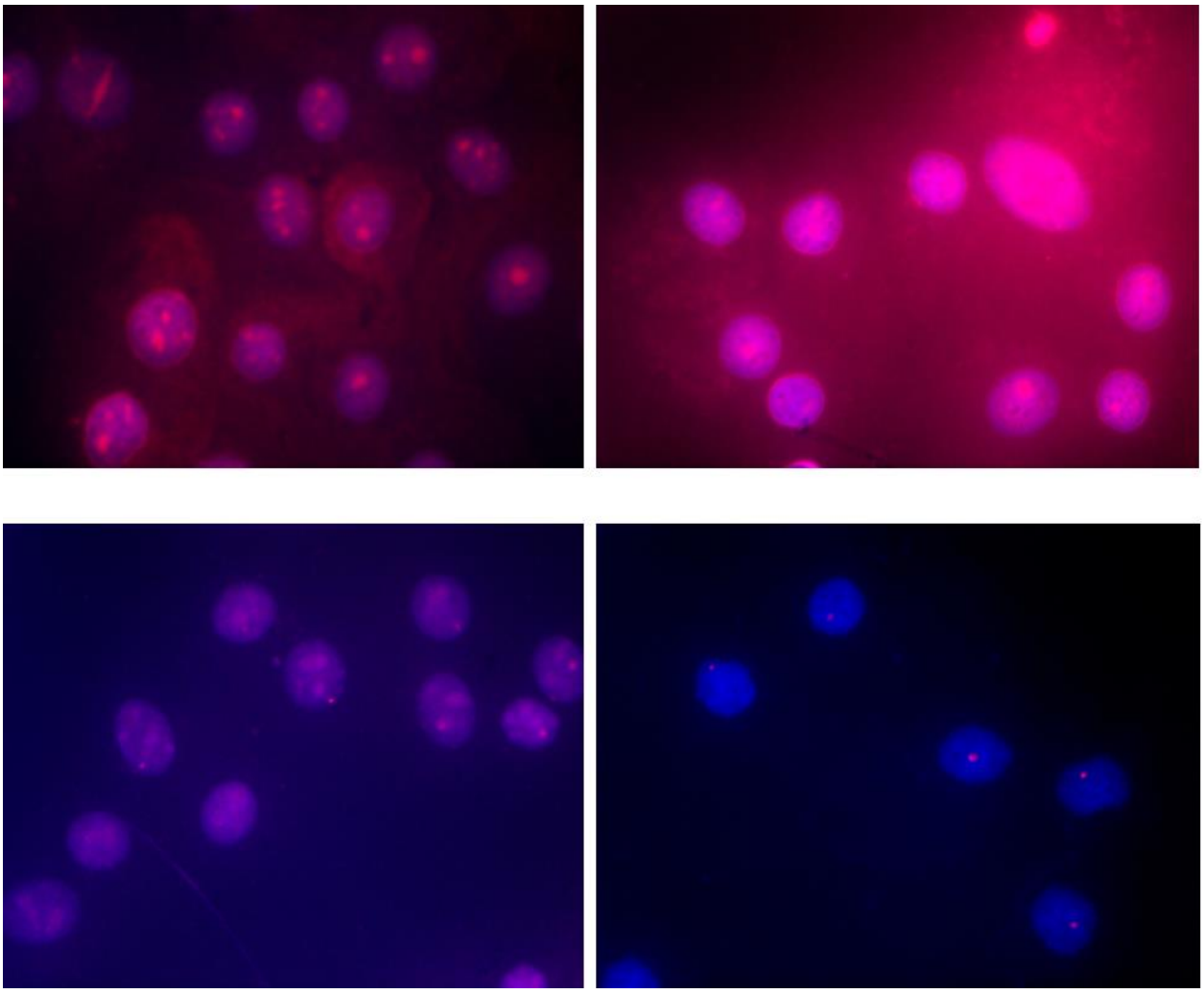

Figure S43. Concentration dependence of **DYZ-OPT**-produced FISH signals under denaturing conditions. Images from FISH experiments using fixed male bovine kidney cells and varying amounts of LNA-modified toehold Invader probe **DYZ-OPT**, i.e., 30 ng (top left), 15 ng (top right), 6 ng (bottom left), and 1.5 ng (bottom right) per 200 µL of 1X PCR buffer. Substantial levels of background signal was observed when **DYZ-OPT** was used in amounts ≥6 ng per 200 µL of 1X PCR buffer. Fixed isolated nuclei from male bovine kidney cells were incubated with **DYZ-OPT** for 5 min at 80 °C in a Tris buffer (20 mM Tris-Cl, 100 mM KCl, pH 8.0) and counterstained with DAPI. Images were obtained by overlaying images from Cy3 (red) and DAPI (blue) channels and adjusting the exposure. Nuclei were viewed at 60X magnification using a Nikon Eclipse Ti-S inverted microscope.

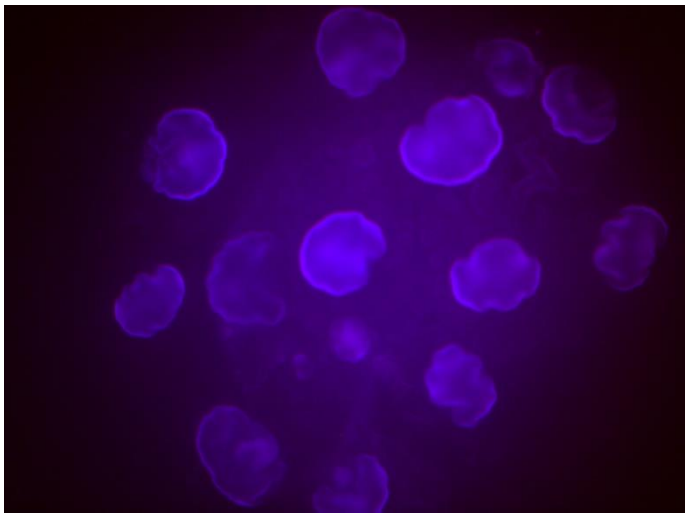

Figure S44. Images from FISH experiments in which LNA-modified toehold Invader probe **DYZ-OPT** was incubated with isolated nuclei from a female bovine endothelial cell line (which lacks the *DYZ-1* target region) under non-denaturing using 15 ng of **DYZ-OPT** per 200 µL of incubation buffer. Conditions are as specified in Fig. 8.

Supplementary references

S1) S. P. Adhikari, R. G. Emehiser, S. Karmakar and P. J. Hrdlicka, *Org. Biomol. Chem.*, 2019, **17**, 8795–8799.

S2) D. C. Guenther, G. H. Anderson, S. Karmakar, B. A. Anderson, B. A. Didion, W. Guo, J. P. Verstegen and P. J. Hrdlicka, *Chem. Sci.*, 2015, **6**, 5006–5015.

S3) S. P. Sau, A. S. Madsen, P. Podbevsek, N. K. Andersen, T. S. Kumar, S. Andersen, R. L. Rathje, B. A. Anderson, D. C. Guenther, S. Karmakar, P. Kumar, J. Plavec, J. Wengel and P. J. Hrdlicka, *J. Org. Chem.*, 2013, **78**, 9560–9570.

S4) S. Karmakar, A. S. Madsen, D. C. Guenther, B. C. Gibbons and P. J. Hrdlicka, *Org. Biomol. Chem.*, 2014, **12**, 7758–7773.

S5) D. M. Crothers, *Biopolymers*, 1968, **6**, 575–584.

S6) H. Ihmels and D. Otto, *Top*. *Curr*. *Chem*., 2005, **258**, 161-204.

S7) D. Andreatta, S. Sen, J. L. P. Lustres, S. A. Kovalenko, N. P. Ernsting, C. J. Murphy, R. S. Coleman and M. A. Berg, *J. Am. Chem. Soc.*, 2006, **128**, 6885–6892.